2005

Joint Center Movement Analysis and 3D Motion Modeling of Upper Arm - Comparison of Several Algorithms with the Visual 3-D Program

Leena Joseph
Virginia Commonwealth University

JOINT CENTER MOVEMENT ANALYSIS AND 3D MOTION MODELING OF UPPER ARM - COMPARISON OF SEVERAL ALGORITHMS WITH THE VISUAL 3-D PROGRAM

A Thesis submitted in partial fulfillment of the requirements for the degree of Master of Science at Virginia Commonwealth University.

By

LEENA JOSEPH
B.E. Biomedical Engineering
Mumbai University, India
July 2002

Director: DR. PETER S. LUM
ASSOCIATE PROFESSOR
DEPARTMENT OF BIOMEDICAL ENGINEERING

Virginia Commonwealth University
Richmond, Virginia
August 2005

Dedication

To my mother and father whose unfailing support and encouragement have been the driving force in my pursuit of higher education. Thank you for being there to celebrate my accomplishment and helping me through the difficult times when success did not come easy. And to my kid brother Jerry whose always cheerful and my biggest ally.

You both are the best parents in the world.

Acknowledgement

I want to acknowledge several people for their help in completing this thesis. I would like to thank my advisor, Dr. Peter Lum for his unwavering support and guidance, but most importantly his immense patience with me throughout my research in the Neuromuscular Rehabilitation Laboratory. He has been a great source of encouragement and has helped me a lot through my study here at VCU.

I want to extend my appreciation to Dr. Paul Wetzel and Dr. Peter Pidcoe for being a part of my thesis committee and making it a reality.

A special thanks to Dr. Karla Mossi for being a constant source of encouragement and helping me out when most required. Also thanks to my friends Azi Saidi and Poorna Mane, thanks for their moral support and help. I also want to acknowledge all the numerous people in my life, who have taught me so much in so many different ways.

Finally, thanks to the staff and faculty of Biomedical Engineering Department for giving me an opportunity to pursue my Master's degree at Virginia Commonwealth University.

Table of Contents

Page

List of Figures

Page

Abstract

JOINT CENTER MOVEMENT ANALYSIS AND 3D MOTION MODELING OF UPPER ARM MOVEMENTS- COMPARISON OF SEVERAL ALGORITHMS WITH THE VISUAL 3-D PROGRAM

By Leena Joseph, B.E. Biomedical Engineering

A thesis submitted in partial fulfillment of the requirements for the degree of Master of Science at Virginia Commonwealth University.

Virginia Commonwealth University, 2005

Major Director: Dr. Peter S. Lum
Associate Professor, Department of Biomedical Engineering

600 out of every 100,000 people in the United States today suffer from some form of cerebellar disease that causes major abnormalities in the equilibrium and aligned, coordinated movement of the body. Hence it becomes essential to diagnose the extent of the movement and gait disorder and provide required therapy to the patients. Various developments have been made in the designing and application of interactive software system for body positioning. Object oriented design techniques are used in the field of software engineering for interactive geometric representation of system behavior. Motion

analysis of the upper and lower extremities of the body could be beneficial in the diagnosis and therapy of numerous orthopedic and neurological ailments. Mathematical models of neuro - musculoskeletal dynamics establish a scientific basis for movement analysis.

As mentioned above, an interactive geometric representation of the system behavior is an important diagnostic tool in orthopedic therapy. This realistic depiction of the human body with respect to the model is a very effective diagnostic tool for clinicians. There are existing biomechanical modeling tools like Visual 3-D etc. that are used for motion analysis. Visual 3-D was developed by the movement disorders laboratory at NIH. The preferred method is to place markers on the segments and calculate the joint center locations using a rigid-body assumption. However studies have shown that markers on the joint centers are subject to artifact (skin movement). Moreover, very few details are provided on the algorithm used by Visual 3-D, and no "fixes" are provided for marker dropout.

This project aims at testing the accuracy of existing biomechanical movement analysis software Visual 3D by calculating the rigid body motion from the spatial co-ordinates of the markers clusters on the subject's upper extremities. This project tries to emulate their approach in a simple and effective manner and at the same time validate the approach by testing it by three different methods by calculating the elbow and wrist locations during a forward reaching motion of the subject. A mathematical model is developed by determining a relationship between the projections of a particular point in

two different planes or on a single plane in two different directions [Kinzel, G.L. et. al. 1972]. The computer simulations are performed using MATLAB to calculate the kinematical parameters from the co-ordinates of projections of markers placed on the upper extremities of the subject's body. This relation will aid in quantitative motion analysis of the upper extremities in the rehabilitation setting. This can be extended to in-depth gait analysis of the lower extremities too. This type of biomechanical movement analysis allows us to understand the dynamic implications of a particular impairment, such as spasticity or weakness, in a particular muscle group.

Chapter 1

Introduction

The use of quantitative body motion and gait analysis in the rehabilitation industry has increased only recently. Gait analysis methodology has been around for over 100 years; however, work to improve gait analysis technology and repeatability has occurred only over the past 10 years. This has been the result of two major factors: a better understanding and interpretation of the information that the measurement systems can provide and the development of more clinically appropriate software for the collection and reduction of data and analysis of results. This has been aided by the rapid development of hardware technology for more efficient clinical biomechanical analysis with faster computing equipment and cameras based on solid state electronics.

Often in the past, the technical details of motion and gait analysis made these *clinical* analyses extremely cumbersome and time-consuming. Kinematical analysis of bone movements in cadaveric specimens and living subjects is a key factor in the study of movement.

1.1. Clinical gait analysis: Current methods and future direction

The innumerable current approaches for the study of human locomotion have provided invaluable insight into the characteristics of normal gait or movement as well as those affected by various neurological and pathological disorders. A typical use of the movement and gait data involves case-by-case analyses with additional efforts in understanding the biomechanical significance of particular deviations from normal patterns or values [Harris, G.F. et. al. 1996]. This evaluation helps clinicians and physiotherapists to diagnose movement disorders and provide the right treatment.

The evaluation of movement and gait analysis of children and adolescents with cerebral palsy constitutes the most prominent use of gait analysis in a clinical environment [Perry, J., 1992, Gage, J.R., 1991]. The clinical research of movement analysis of subjects suffering cerebral palsy includes assessment of the pre-operative and post-operative changes in motion/gait associated with different surgical procedures. Other applications of movement analysis include the evaluation of subjects with motion impairments occurring as a result of myelomeningocele [Thomas, S.E., et. al. 1989], stroke [Olney, S.J., et. al. 1986], Parkinson's disease [Blin, O., et. al. 1990], postpolio sequelae [Maynard, F.M., et. al. 1985] and amputations [Hurley, G.R., et. al. 1990].

In subjects suffering from hemiplegia cerebral palsy, 3D motion analysis is performed during various tasks such as reaching and grasping. These analyses can be performed before and after tendon transfer surgery with or without the aid of Botulinum

Toxin injections. A biomechanical model can be used to describe the movement patterns resulting from spastic hemiplegia and eventually predict accurately the functional changes in the upper extremity movement patterns after surgical or pharmacological treatment. Similarly, 3D motion analysis system can be utilized to keep a track of the movement improvement in diplegic cerebral palsy children.

1.2. Why computer/numerical analysis?

Computer simulation and modeling have contributed much to the understanding of a wide range of biomedical phenomena. Numerical analysis is a very powerful tool in the field of engineering, applied mathematics and mechanics and medical sciences. The use of numerical techniques is very essential for problem-solving involving complex geometry and physical properties that arise in biomechanics. The enhanced speed and expanded storage capacity of the modern computers, combined with recent advanced numerical programming and computing techniques have vastly improved the potential for studying complicated biomechanical processes. With the rapid growth in technology, three dimensional (3-D) motion analyses has developed into a sophisticated research tool and an immense aid in preoperative planning and post operative assessment. Technical advances in data collection, storage and output have greatly reduced the time and human labor involved in making the results of clinical studies available for assessment of individual patients.

1.3.Thesis Organization

The biomechanical modeling of upper arm movements utilizing data from the video images of marker clusters on the arm consists of 4 chapters.

Chapter 1 offers an introduction to the existing gait analysis methods and the role of numerical computations in it. Chapter 2 gives an in- depth review of the background of human motion analysis. Chapter 3 puts forward the modeling approach along with the principle of a biomechanical construction, the measurement methods and the various analysis techniques. Chapter 4 shows the results obtained by basic kinematical approach, its cross verification and the effects of alternate compensations to this elementary method. It analyses and discusses them after validating it.

Appendix A provides a brief description of the joint mechanics and the movements. Appendix B lists all the program codes that have been implemented. Appendix C is a glossary of all the medical conditions that occur in this thesis.

Chapter 2

Background

One out of every 300 people in the world today suffer from some form of cerebellar disease that causes major abnormalities in the equilibrium and aligned, coordinated movement of the body. Hence it becomes essential to diagnose the extent of movement and gait disorder and provide required therapy to the patients. Movement analysis is extremely useful in pre-operative assessment and can provide invaluable insight into subtle functional musculoskeletal adaptations. There are two types of movements in humans: voluntary movements such as walking, sitting, etc. that are under our control and happen on our own accord and involuntary movements like chorea, ataxia and tremors that are associated with certain medical abnormalities. The most prevalent medical condition that leads to movement disorders is Parkinson's disease. It can result in involuntary tremors of the upper extremities. Huntington's disease and Cerebellar disease also cause involuntary movements or tremors in the body.

An understanding of movement disorders requires the knowledge of joint movements in the human body. This study of movements in the joints of the human body is an example where changes in position of one skeletal part in relation to another similar part have been studies for years using various methods. These biomechanical studies

represent important aspects of functional anatomy. They are also essential in clinical work. Biomechanical analyses of these magnitudes require essentially the following two factors:

1) Well defined concepts of the two basic forms of motion i.e. rotation and translation.
2) Accurate methods for measuring the movements of the skeletal segments.

2.1. History of Human Motion Analysis

Human motion analysis forms the basis for various clinical and research applications. A perfect blend of clinical assessment and computed movement analysis can be a powerful tool for a clinician or researcher. The art and science of motion analysis has expanded from the basic descriptions of ambulatory patterns to play major front-line clinical roles in surgery, rehabilitation, prosthetics, orthotics, surgery, ergonomics and athletes.

Since the beginning, human movement has been observed and analyzed. The relation between motion and muscle was appreciated by the Greeks and is mentioned in the book *On Articulations* by Aristotle [Basmajian, J.V., 1978]. This work on movement analysis continued over the centuries until 1836 when W. Weber and E. Weber began their scientific investigation of the mechanics of human gait. Their analysis included measurement of stance and swing phases, trunk movements, step duration, and step length [Steindler, A., 1970]. This was followed closely in 1881 when V. Vierordt studied the development of kinematics by analyzing foot print patterns with colored fluid projections. Photographic techniques using light stripes attached to the body parts were introduced in

the1800's by E. Marey. Simultaneously, E. Muybridge introduced the use of cameras triggered sequentially to record motion during gait [Muybridge, E., 1887]. In 1895, W. Braune and O. Fischer introduced mathematical computations to calculate the velocities, accelerations and forces during gait [Harris, G.F., 1996].

Movement analysis has played a major role in the advancement of surgical treatment of subjects with cerebral palsy. It has proved very useful in the study of neuromuscular disorders [Olney, S. J. et. al.1991], the evaluation of joint replacements and the study of athletic injuries, amputees, orthotics and other assistive devices. Although simple observational analysis of movement characteristics by a trained clinician is sufficient, recent advances in bioengineering have enabled precise analysis of specific characteristics like joint angles, angular velocities and acceleration (kinematic analysis), joint forces, moments and power (kinetic analysis).

2.2. Rigid Body Motion

2.2.1 Classification of Motion

Despite the large variations in the way human beings move, movements can be described into translatory, rotational or a combination of the two motions. The latter form of motion is termed as the general form of motion [Trew, M. et. al. 1997].

➢ **Translatory Motion**

A motion that moves all points of a body on a straight line over identical distances is termed linear motion or translation. In translatory motion, all points on the body follow a parallel path such that the orientation of the moving body remains constant. Translation can be:

- Linear / Rectilinear; Body moves along a straight line.

  Example: The motion undergone by a wheelchair occupant while being pushed along a level floor as shown in Figure 2.1.

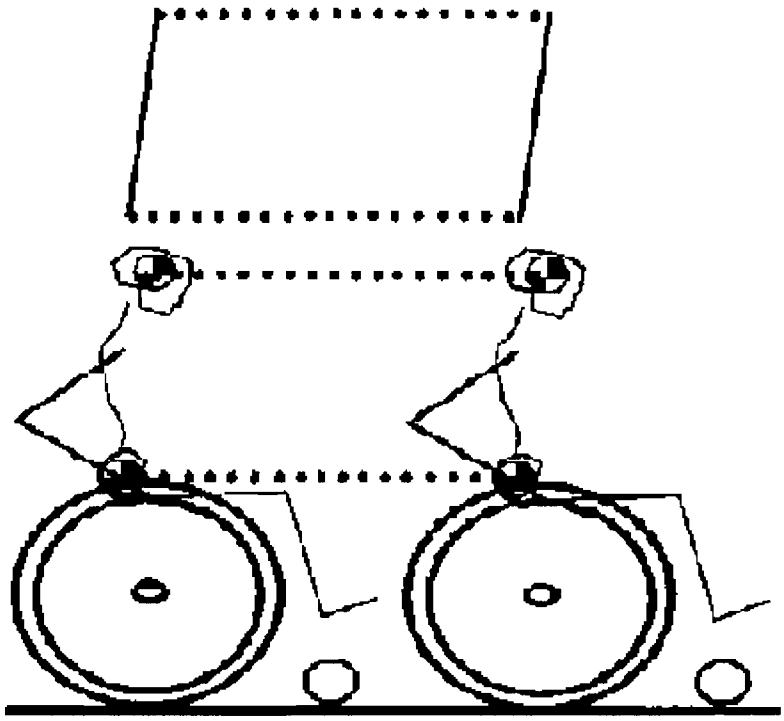

Figure 2.1. Rectilinear motion of a person on a wheel chair [Trew, M. et. al. 1997].

- Curvilinear; Body moves along a curved path.

  Example: The motion of the trunk of a subject when stepping down from a step as shown in Figure 2.2

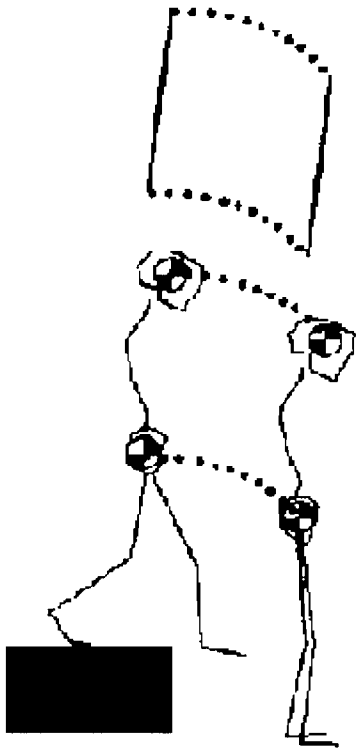

Figure 2.2. Curvilinear motion of a person stepping down from a block [Trew, M. et. al. 1997].

- **Rotational/Angular Motion**

A motion that moves all points of a body in independent circular paths about a common fixed axis is termed as rotational motion. In angular motion, all parts of the body move through the same angle in the same time.

- **Translation and Rotational Motion**

A combination of translation and rotational motion is termed as general body motion as shown in Figure. For example the whole body undergoes translatory motion as a result of the rotational motion occurring around the joints of the lower limbs.

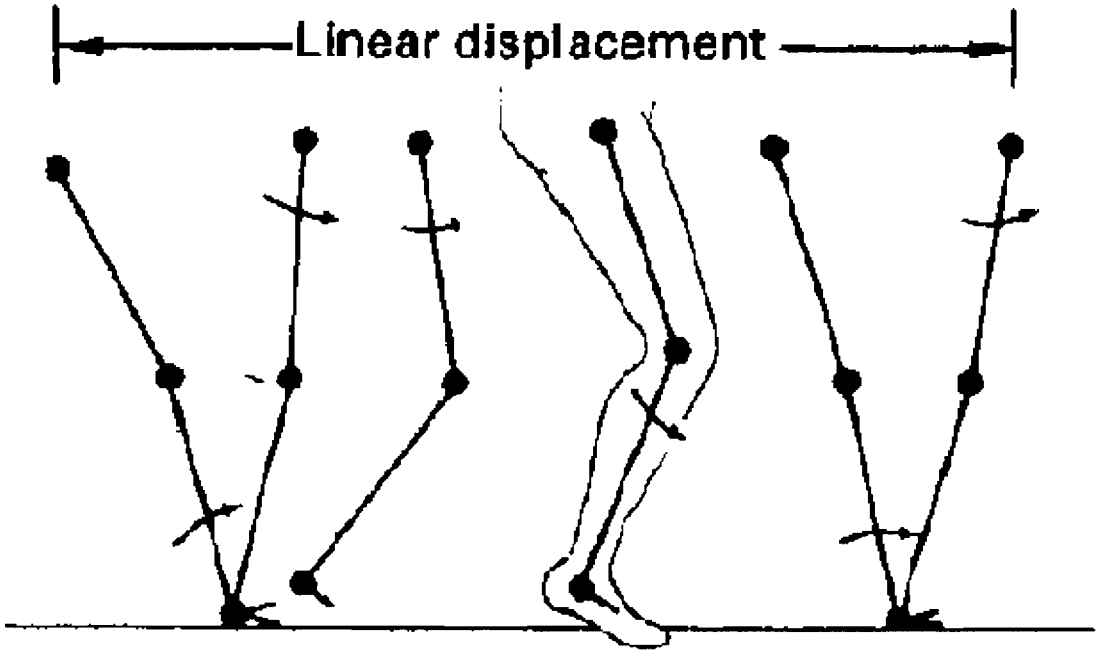

Figure 2.3. General plane motion

2.2.2 What is a Rigid Body?

A rigid body is defined as a system of particles in which the distances between the particles do not vary. They remain constant throughout the duration of motion of the system. Non rigid bodies or deformable motion description is a very complex task. The rigid body is a mathematical model of the behavior of some physical bodies. The main advantage of the rigid body model is that motion can be described by using few parameters, and thus correspondingly the motion can be determined by only a few measurements.

- Conditions for stability of a rigid body [Trew, et. al. 1997]

The stability of a rigid body depends on the following conditions:

- The area of the base of the support.
- The height of its center of gravity above the base.
- The weight of the body.
- The position of the line of gravity relative to the base of support.

The state of balance of the human body can be improved if it is made more stable. It becomes more stable when:

- The center of gravity of the total weight supported over the base is lowered. The total weight will include any additional weights being carried.
- The total weight of the body and any weights being carried are increased.
- The center of gravity is directly above the center of the base of support.
- The area of the base of support is enlarged.

2.2.3 History of the kinematics of rigid body

Newton (1643-1727) is known as the father of analytical mechanics with the highlight of his study being mechanics of mass points. He described universal gravitation and, via his laws of motion, laid the groundwork for classical mechanics. It took approximately 400 years since the groundbreaking works of Brahe, Kepler and Galilei for classical mechanics to develop.

Classical mechanics is one of the major sub-fields of study in the science of mechanics, which is concerned with the motions of bodies and the forces that cause them [36]. Classic mechanics is an in-depth model of the physics of forces acting on a body and causing its motion. As mentioned above, it is also referred to as 'Newtonian Mechanics' after Newton and his laws of motion. Classical mechanics can be further classified into the following types:

1) Statics

   This is the study of objects at rest.

2) Dynamics

   This is the study of objects subjected to external forces.

   2a) Kinematics

      This is the description of motion in precise mathematical terms without reference to the forces producing the motion.

   2b) Kinetics

This is the description of forces affecting motion of body in a particular manner

However the fundamental theorems of the motions of the bodies with extension in space were the result of Euler's (1707-1783) work [Euler, L., 1776].

2.3. Modeling the Human Body

Mechanics is the study of the motion of material bodies. As mentioned above, the description of motion in mathematical terms is called kinematics and is independent of the cause of the motion. The study of motion is called kinetics or dynamics. An important aspect of dynamics is statics, or the lack of motion due to various causes.

As mechanical systems go, the human body is a very complicated creation that can be considered rigid. Our human body can be considered as a 3-D mechanism with many degrees of freedom. It is actuated by hundreds of muscles, and many movements involving changing boundary conditions and contact problems. Bones can be considered as segments of the rigid body. This is because the motion of a rigid body in a system is similar to elements like anatomical bones because essentially the distance between two bones does not vary.

2.4. Rigid Body Motion

Some of the various movements performed on a daily basis are locomotion such as walking and running, upright posture control, limb movements such as reaching and manipulation and sporting movements like tennis and basketball. All these activities are characterized by the fact that a multiple-degrees-of-freedom system of the musculoskeletal system is controlled. The human body can be considered as a redundant system having more than 100 joint-degrees of freedom and a complex non-linear dynamic system. In order to understand and achieve smooth movements, these redundant joint-degrees of freedom must be constrained [Ito, K., et. al. 1991].

The degrees of freedom of a rigid body are defined as the number of parameters needed to define the position of the rigid body in space. The number of degrees of freedom for any segment is six; three degrees of freedom of translation that define position and three degrees of freedom of rotation that define orientation.

2.5 Initial Biomechanical Work

In studies conducted by the German scientists Braune and Fischer in 1885 on the motion of skeletal segments, they were treated as rigid bodies. The motion of the segment as a whole was studied and not the various mass points in the segment. In order to study the motion of a rigid body, it is sufficient to determine the motion of minimum three non collinear points on the body. The screw motion is calculated. By direct measurements they

determined the indicators, attached to the radius or ulna during the motion of an arm of a specimen.

The measurements were made in a laboratory coordinate system, two axes of which were defined by a horizontal millimeter paper. The position on the third axis was determined on a plumb line from the point to be measured to the horizontal paper. This is considered as the first attempt to determine true three dimensional coordinates during the movement of an object. This further enabled the study of rigid body motion and its parameters from measured positions of points by various computational methods in the coming years. Braune and Fischer later on utilized photogrammetry to determine positions in space of markers.

2.6. Displacement of a Rigid Body

The rigid body has two fundamental forms of displacement i.e. translation and rotation. Translation is a displacement in which every point of the body undergoes the same amount of movement. Rotation is a displacement such that the points lying along a line around the same rotation axis remain unchanged with respect to the line. The system of mass points outside the line move in proportion to their distances from the line. The turning of an object or co-ordinate axes about a fixed point is also termed as rotation. A rotation is an orientation preserving orthogonal transformation.

Euler proved that the general displacement of a rigid body with one fixed point is a rotation about an axis through this point. A corollary to this theorem is that the general displacement of a rigid body is the sum of the translation of a base point and a rotation about this base point. This is so because by definition, translation is the displacement of one point. He proved that the rigid body displacement is represented by a transformation given by:

$$\bar{r} = M\bar{r}_0 + \bar{d} \qquad \text{(a)}$$

Where $\bar{r}$ = New position vector of every point in the rigid body after motion

M = Rotation matrix

$\bar{r}_0$ = Original position vector of every point in the rigid body

$\bar{d}$ = Translation vector

The translation vector $\bar{d}$ is dependent on the different choices of base point, whereas the rotation matrix is independent of the base point. An expression for the translation $\bar{d}_p$ of a another base point P, is obtained if we substitute $\bar{r}_0$ by $\bar{r}_{OP}+\bar{r}_0$ where $\bar{r}_0$ is the vector relative to P for a point in the body.

$$\bar{r} = M\left(\bar{r}_{OP} - \bar{r}_0\right) + \bar{d} \qquad \text{(b)}$$

$$\bar{r} = M\bar{r}_0 + \bar{d} + M\bar{r}_{OP} \qquad \text{(c)}$$

Since $\bar{d}' = \bar{d} + M\bar{r}_{OP}$, (d)

$$\bar{r} = M\bar{r}'_0 + \bar{d}' \qquad \text{(e)}$$

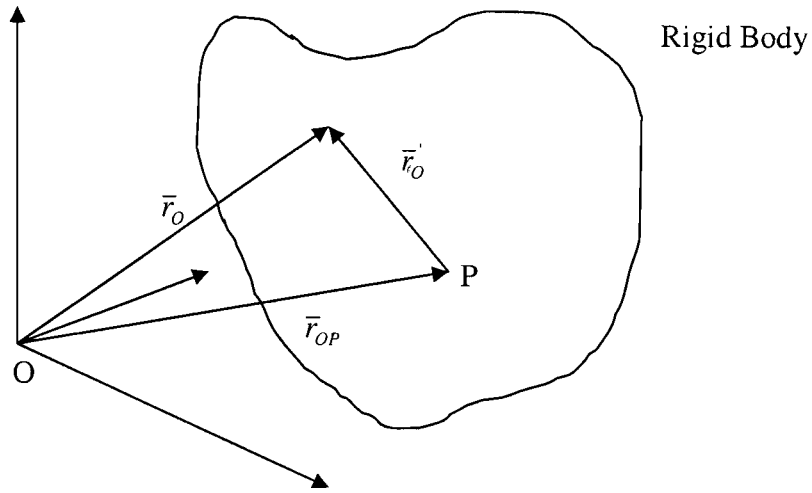

Figure 2.4. Position vector r_0 in relation to a base point P [Selvik, G., 1989]

This proves that the change of position of a point P:

$$\bar{d}_p = \bar{d} + (M - I)\bar{r}_{OP} \quad \text{.....where } I \text{ = Identity Matrix} \qquad \text{(f)}$$

It also proves that the rotation matrix is independent of the base point.

Chapter 3

Modeling Approach

3.1. Determining Rigid Body Transformation

In many biomechanical analyses it is essential to determine the rigid body transformation parameters; parameters which describe the transformation of points from one reference frame to another. These parameters are a scale factor, rotation matrix and a position vector. The scale factor allows these parameters to be used to describe the transformation required to map points between reference frames of different scales. One application of scaling of this sort is osteometric scaling, which allows the locations of the origins and insertions of muscles and ligaments that are inaccessible on a live subject, and therefore not easily measurable, to be obtained from the results of cadaveric dissection and measurement [Challis, J., 1995]. It has been proved that the direct application of dry bone data to a live subject is inappropriate and that some form of scaling is necessary as the chances of the physical dimensions of the bones of the cadaver and the experimental subject being different are highly possible [Lew, W. D., et. al. 1977]. Various modifications have been made to this method for biomechanical analysis with the introduction of identical extent of differing amounts along three mutually orthogonal axes (x, y and z) defined in both the rigid bodies. But none of the methods take into account of

the errors in the measured positions of landmarks on either the specimen or the experimental subject.

If the scale factor is equalized to unity and the rotation matrix is orthogonal, then the rigid body transformation parameters can be used to describe the position or orientation or movement of a rigid body. Spoor and Veldpaus (1980) proposed a technique for measuring the rigid body parameters by minimizing a least squares algorithm by calculating the eigen vectors and eigen values of a three by three matrix [Spoor, C.W. 1980]. This was further modified to measure the rigid parameters without using eigen vectors [Veldpaus, F.E. et. al. 1988]. We are utilizing this technique to provide a computational design to determine the rigid body transformation parameters.

3.2. Principle of Model Construction

The approaches to determine the rigid body motion include utilizing the co-ordinates of atleast three non-coplanar points in order to calculate the respective matrices that describe both rotation and translation [Kinzel, G.L., et. al. 1972]. In the case of markers less than three, Chao et. al. calculated the rotation matrix R from two vectors, pointing from one of three markers to the other two [Chao, E.Y., et. al. 1978]. In our approach which is along the lines of Selvik [Selvik, G., 1974], the different upper extremities are divided into segments and a flexible biomechanical model can be utilized to link together these different segments in a coherent manner. The resultant biomechanical model allows the end user to perform analyses on the acquired movement data. The end

user has control over the coherent linking and analysis of the various segments and structures. This enables us to study and understand the upper and lower mannerisms such as head movements, moving the arms and fingers, wheel chair locomotion, throwing motions, etc. Diagnosis and treatment of numerous neurological and orthopedic disorders could benefit from motion analysis of upper and lower torso.

The upper body extremities are divided into segments for ease. Each segment is composed of joints, with each joint being composed of six degrees of freedom. Degree of Freedom (DoF) is a single coordinate of relative motion between two bodies. Such a coordinate is free only if it can respond without constraint or imposed motion to externally applied forces or torques. For translational motion, a DoF is a linear co-ordinate along a single direction. For rotational motion, a DoF is an angular coordinate about a single, fixed axis. Three non-collinear markers attached to the segments can determine these 6 degrees of freedom.

A marker based measurement procedure is adapted to calculate the position of any segment of the body in space. The motion of rigid segments in space can be determined by measuring the degree of freedom of the concerned of the concerned segments. This is achieved by measuring the 3 independent translational DoF (defining position) and the 3 independent rotational DoF (defining orientation). From these 6 parameters we can obtain the location of the particular segment in space.

3.3. Degrees of Freedom Calculation

A biomechanical skeletal model that comprises the relative location of all the defined segments and their coordination with the adjacent segments has to be constructed. Three or more non-collinear markers or targets are considered for each segment and their position is defined in the orthogonal local segment coordinate system (SCS). These markers are located independently within each segment. In addition to this we also define the position of the markers for a global frame of the system called as orthogonal global laboratory coordinate system (LCS).

These three non collinear markers or reference points help in defining the six degrees of freedom associated with the position and spatial orientation of the body segment. This orientation can be described through the computation of three independent absolute angles. Once the absolute orientation of each segment is obtained, the spatial orientation of one segment relative to another may be computed. These relative angles are referred to as joint angles, and also known generally as kinematics. The kinematic parameters are calculated using the least-squares algorithm by Spoor and Veldpaus [Spoor, C. W., et. al. 1980]. This rigid body motion can be calculated from spatial co-ordinates of markers placed on the extremities. The only condition imposed is that the number of targets/ markers should be more than or equal to zero to reduce the erroneous readings.

3.4. Measurement Procedure

The most common method of gathering information that is associated with the position of body segments and joints is through the use of external markers placed on the subject that are tracked with the multi camera systems [Whittle 1991].

The first step involved in biomechanical analysis is to place the makers on the body segments and align it with specific bony landmarks. The motion of these target markers attached to the subjects arm is recorded. This recording will be done with the help of high-speed cameras and a high-resolution data acquisition system. This displacement of the markers, which are either passive (retro-reflective) or active (light-emitting diodes) is simultaneously viewed and recorded by two to seven cameras. Stereo metric techniques [Woltring, H.J. et. al. 1990] are used in a frame-by-frame analysis to combine the two-dimensional camera images and determine the instantaneous three-dimensional co-ordinates of each marker relative to the fixed laboratory co-ordinate system (LCS).

3.4.1 Upper Extremity Measurement Setup

A minimum of three markers are required to determine the rigid body motion from the video images of marker clusters. In this project four markers are utilized. The markers for the upper arm include; an upper arm lower lateral marker ALL, an upper arm lower medial marker ALM, an upper arm upper lateral marker AUL and an upper arm upper medial marker AUM. Similarly the four target utilized for the motion measurement of the

forearm comprise; a forearm lower lateral marker FLL, a forearm lower medial marker FLM, a forearm upper lateral marker FUL and a forearm upper medial marker FUM.

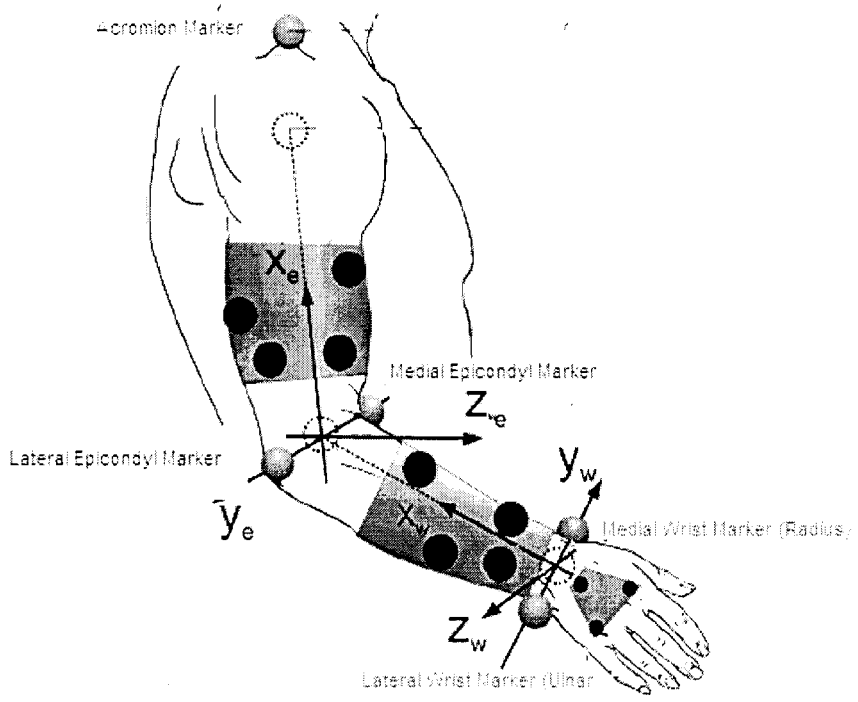

Figure 3.1 Marker arrangement on the upper arm with the respective axes [Schmidt, R., et. al. 1999]

This is shown clearly in the Figure 3.1. The joint centers are defined with additional markers at the medial and lateral epicondyl and medial (radial) and lateral (ulnar) to the wrist axis. The joint center of the wrist at the time of static calibration measurement is the middle between the ulnar and the radial wrist markers. Similarly the joint center of the elbow is the middle between the medial and lateral elbow markers. The shoulder center is assumed to be 7cm inferior to the acromion marker.

The technology associated with the measurement approach plays an important role. The applications of solid state electronics have improved the camera hardware characteristics. Host computer requirements for the measurement systems have been reduced and at the same time personal computer efficiency has increased. The computing costs associated with motion measurement systems have come down while maintaining sufficient speed for data collection and processing,

Passive marker measurement systems such as ViconPeak (Oxford Metrics, Ltd., Oxford, England), ExpertVision (Motion Analysis Corporation, Santa Rosa, California), and Peak Performance (Peak Performance Technologies, Englewood, Colorado) use light sources placed very near each camera to generate light, which is reflected from the highly reflective markers that are usually small spheres [Harris, G.F., et.al.1996]. Active marker systems such as Selcon (Selspot Systems, Ltd., Southfield, Michigan) and Optotrak (Northern Digital, Inc., Waterloo, Ontario, Canada) use small light emitting diodes (LED's) placed directly on the subject to generate the light that is recorded by the motion cameras. The advantage of the active marker system is that the anatomical location of each marker is known because the LED's are sequentially pulsed by the control and data acquisition system. This is an important factor because of the time saved in the data reduction. The operator of the passive maker system assists the computer with marker identification. The disadvantage of this technique is that there is are strong chances of subject distraction and movement alteration because the system of cables that powers and

controls the LED's trails the subjects as they move and the potential for "phantom marker artifacts" due to reflection of LED pulses testing surfaces such as the floor.

The data collected from the multiple movement trials is a series of frames of data with each frame containing the 3-D locations of the external markers at that instant in time. This the 3-D path of each marker, generally referred to as trajectory is measured. The spatial relationship between markers placed on the same body segment defines the orientation of that body segment in space. The biomechanical model give details regarding the number of segments involved, the joint properties and other kinematical parameter calculation. To determine this, transformation between the tracking markers placed on the subject's arm will be done on to the designed model. Data obtained from the transformation can be used to further calculate orientation angle of the joints of the body, the joint center of location, etc. This can be utilized to interpret specific movement disorders. This is a future addition to the project that will complete the biomechanical model.

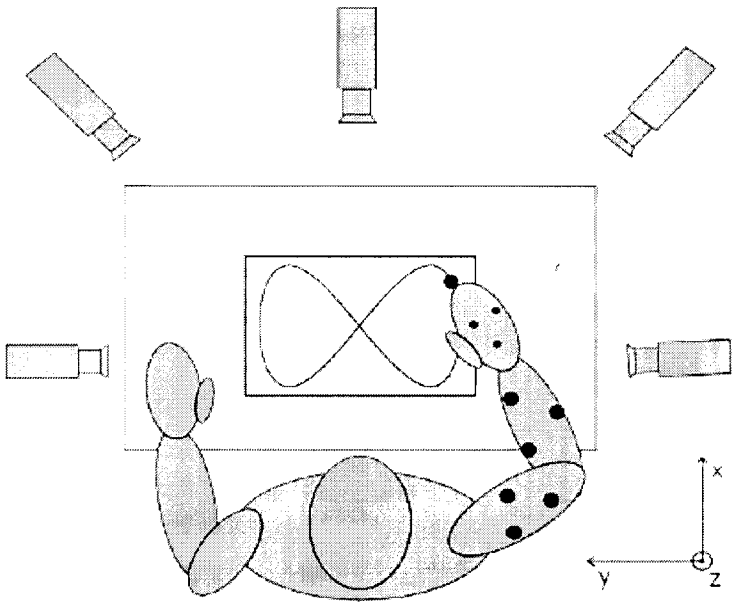

Figure 3.2. View from above of the setup of tacking task [Schmidt, R., et. al. 1999]

3.5. Analysis

Consider three non-collinear markers/landmarks placed on the upper arm and determine their spatial co-ordinates before and after movement. Obtain the position of the markers before movement and after movement. Spatial co-ordinates of markers in or on bone can be calculated from the coordinates of projections of these markers in two different directions on one or two planes. These spatial coordinates are used to determine the kinematical parameters. This movement of the segment of the body with respect to the markers is described with the help of a rotation matrix and a translation vector or by the position of the screw, the angle of rotation about this axis and the translation along the axis [6]. The calculation of these parameters can be done by minimizing the least squares

method. This implies that a rotation matrix R and a translation vector v can define the movement of the rigid body segment from a position 1 into another position 2. The only condition on this analysis is that the rotation matrix R has to be orthogonal and satisfy the condition.

$$R^{-1}R = R^{T}R = I \tag{1}$$

Where

R – Rotation matrix from the SCS to the LCS

R^{T} – Transpose of the Rotation matrix

R^{-1} – Inverse of the Rotation matrix

I – 3*3 Unity matrix

If we consider a point A on a segment in the orthogonal segment local coordinate system (SCS), then the location of another point P on a segment in the global frame of the system i.e. orthogonal laboratory coordinate system (LCS) is given as

$$P = RA + v \tag{2}$$

For a certain position of a marker, if the rotation matrix R and the translation vector v are calculated, then the SCS co-ordinates of the marker can be determined from the measured value of P as:

$$A = R^{-1}[P - v] \tag{3}$$

For every new position of marker A, the rotation matrix R and the translation vector v can be determined by measuring the global position P. This analysis is based on the minimization procedure of the least square algorithm by Selvik et. all which states

$$\sum_{i=1}^{m} \left(\left(P_i - RA_i\right) - v\right)^2 i \qquad (4)$$

Where m - Number of markers/landmarks used

The condition imposed on the number of markers is that it should be equal to or more than three.

Let a_1, a_2, a_3, $a_4 \ldots . a_n$ denote the radius vectors of n non-collinear points $(n \geq 3)$, P_1, P_2, P_3, $P_4, \ldots . P_n$ of the body in position 1 (before movement). As per the above stated theory, the new radius vectors q_1, q_2, q_3, $q_4, \ldots . q_n$ of these points in position 2 (after movement) are defined as

$$q_i = Ra_i + v \qquad (5)$$

for $i = 1,2,3,\ldots .n$

The rotation matrix R and the translation vector v are determined from the measured radius vectors p_1, p_2, p_3, $p_4, \ldots \ldots p_n$ of n non-collinear points $(n \geq 3)$, P_1, P_2, P_3, $P_4, \ldots . , P_n$ of the body in position 2 (after movement). These calculated theoretical values of p_1, p_2, p_3, $p_4, \ldots \ldots p_n$ will differ from the exact vectors q_1, q_2, q_3, $q_4, \ldots \ldots q_n$.

An overall measure of the position vectors difference is defined by the function f as

$$f(v,R)=\frac{1}{n}\sum_{i=1}^{n}\left(Ra_i+v-p_i\right)^T\left(Ra_i+v-p_i\right) \tag{6}$$

This can be further expressed as

$$a=\frac{1}{n}\sum_{i=1}^{n}a_i \tag{7}$$

$$p=\frac{1}{n}\sum_{i=1}^{n}p_i \tag{8}$$

$$M=\frac{1}{n}\sum_{i=1}^{n}\left(p_i a_i^T\right)-pa^T \tag{9}$$

$$f_0^{'}=\frac{1}{n}\sum_{i=1}^{n}\left(a_i^T a_i+p_i^T p_i\right)-\left(a^T a+p^T p\right) \tag{10}$$

Where

a : average of $a_1, a_2, a_3, a_4, \ldots\ldots, a_n$

p : average of $p_1, p_2, p_3, p_4, \ldots\ldots, p_n$

$a_i\ (i=1,2,\ldots\ldots n)$: Radius vector of marker i before the movement

$p_i\ (i=1,2,\ldots\ldots n)$: Measured radius vector of marker i after the movement

$q_i\ (i=1,2,\ldots\ldots n)$: Exact radius vector of marker i after the movement

n : Number of markers

M : Matrix of order 3*3

$f_0^{'}$: Scalar quantity

This expression for f_0 can further be written as:

$$f(v,R) = f_0 + (Ra + v - p)^T (Ra + v - p) - 2trace(M^T R) \quad (11)$$

The component $trace(M^T R)$ is equal to the sum of the components on the main diagonal of the 3x3 matrix $M^T R$.

The Lagrangian multiplier theorem is used to determine the matrix R and the translation vector v that minimize f under the constraint condition as per equation (1). A 3*3 matrix S of Lagrangian multipliers and a function F of v, R and s is introduced to use the Lagrangian theorem.

$$F(v,R,s) = f(v,R) + trace(S(R^T R - I)) \quad (12)$$

Equation (12) states that, if $F = F(v,R,s)$ is stationary for some v, R and s; then $f = f(v,R)$ is stationary and the condition (1) is satisfied for that v and R. The first order derivative δF of the function $F(v,R,S)$ has to be zero for each order derivative $\delta v, \delta R$ and δS of v, R and s in order to calculate the stationary points of $F = F(v,R,s)$.

$$\delta F = 2(Ra + v - p)^T (\delta R a + \delta v) - 2trace(M^T \delta R) + trace(\delta S(R^T R - I)) + trace(S(\delta R^T R + R^T \delta R)) \quad (13)$$

Let us consider each derivative. Equalizing $\delta F = 0$ for δS, results in the orthogonality condition in equation (1). Equalizing $\delta F = 0$ for δv, gives and equation for v.

$$v = p - Ra \tag{14}$$

Equalizing $\delta F = 0$ for δR, along with equation (14) and $trace\left(S\delta R^T R\right) = trace\left(S^T R^T \delta R\right)$ gives us the equation for matrix M

$$M = \frac{1}{2} R\left(S + S^T\right) \tag{15}$$

Equation (11) is solved to calculate the symmetric matrix $\frac{1}{2}\left(S + S^T\right)$. We know that

$$\overline{S} = \frac{1}{2}\left(S + S^T\right) \tag{16}$$

Also $M = R\overline{S}$ (17)

From equation (1), (16), (17) we get;

$$\overline{S}^2 = \overline{S}^T R^T R\overline{S} = M^T M \tag{18}$$

We analyze the calculated matrix M to obtain a symmetric matrix defined by $M^T M$ that has Eigen values $D_{11}^2 \geq D_{22}^2 \geq D_{33}^2 \geq 0$ and corresponding set of three orthonormal vectors. The Eigen values are arranged on the principal diagonal of a diagonal matrix D^2 while the Eigen values are considered as the columns of a 3*3 matrix V. This satisfies the condition;

$$M^T M = \overline{S}^2 = VD^2V^T \tag{19}$$

Such that $VV^T = I$ (20)

The solution for the symmetric matrix $\overline{S}$ is calculated as

$$\overline{S} = VDV^T \tag{21}$$

where the signs of the principal diagonal components D_{11}, D_{22} and D_{33} are indeterminate.

Combining equation (15) and (17) gives;

$$M = RVDV^T \tag{22}$$

The rotation matrix R can be calculated from equation (22) if and only if at least two of the Eigen values $D_{11}^2 \geq D_{22}^2 \geq D_{33}^2 \geq 0$. This is possible if and only if three or more non collinear points are being used. The coefficients of the matrix MV are calculated to give;

$$RVD = MV = [m_1 \quad m_2 \quad m_3] \tag{23}$$

where

$m_i (i = 1,2,3)$: represents column i of MV

M : Matrix of order 3*3

D : Diagonal matrix of square roost of Eigen values of $M^T M$

V : Orthogonal matrix of Eigen vectors of $M^T M$

R : Rotation matrix

Since D is a diagonal matrix, m_i is equal to the column i of RV, and multiplied by D_{ii}. In a realistic situation, the value of D_{11} and D_{22} should not be zero. This implies that column 1 and column 2 of RV are equal to $\left(\frac{1}{D_{11}}\right).m_1$ and $\left(\frac{1}{D_{22}}\right).m_2$ respectively.

Since RV is orthogonal, the column 3 of RV is equal to the cross product

$\left(\frac{1}{D_{11}.D_{22}}\right) m_1 * m_2$ of the column 1 and column 2.

Thus the final equation to calculate the rotation matrix R is

$$R = \left(\frac{1}{D_{11}} m_1 \quad \frac{1}{D_{22}} m_2 \quad \frac{1}{D_{11}.D_{22}} m_1 * m_2 \right) . V^T \tag{24}$$

The translation vector can be calculated from the equation (14)

$$v = p - Ra$$

3.6. Determination of Helical Axis

As described above the movement of the body is characterized by the rotation matrix R and the translation vector v. From classical mechanics we know that it can also be considered as the result of a rotation through an angle Φ about the helical axis and a translation t along this axis. If we consider a unit vector n acting along the helical axis and s to be the radius vector of a point on this axis such that s and n fulfill the condition of orthogonality, then;

$$\begin{aligned} n^T n &= 1 \\ n^T s &= 0 \end{aligned} \tag{25}$$

The direction of n and the sense of rotation correspond to the right hand screw rule. Φ will always be non- negative and less than or equal to π radians.

The connection between both descriptions of the movement of the body is given by the requirement that the below equation must be true for every vector w.

$$Rw + v = w + tn + (1 - \cos\Phi)n * (n * (w - s)) + \sin\Phi n * (w - s) \tag{26}$$

Solving the above equation

$$v = tn + (1 - \cos\Phi)s - \sin\Phi n * s \tag{27}$$

For every value of w, the following is true

$$Rw = \cos\Phi w + (1 - \cos\Phi)nn^T w + \sin\Phi n * w \tag{28}$$

This is equalized for every value of w to

$$\frac{1}{2}(R - R^T)w = \sin\Phi n * w \tag{29}$$

$$\frac{1}{2}(R + R^T) = \cos\Phi I + (1 - \cos\Phi)nn^T \tag{30}$$

The defined matrix $\frac{1}{2}\left(R - R^T\right)$ is skew - symmetric and it can be easily shown that

$\sin\Phi n$ is given by:

$$\sin\Phi n = \frac{1}{2}\begin{bmatrix} R_{32} - R_{23} \\ R_{13} - R_{31} \\ R_{21} - R_{12} \end{bmatrix} \tag{31}$$

From (25) we know that n is orthogonal and $\sin\Phi n \geq 0$ .The above equations can be solved to obtain the trigonometric functions $\sin\Phi$ and $\cos\Phi$.

Equation (31) can be solved to obtain the value of $\sin\Phi$:

$$\sin\Phi = \frac{1}{2}\sqrt{(R_{32}-R_{23})^2+(R_{13}-R_{31})^2+(R_{21}-R_{12})^2} \tag{32}$$

Equation (30) can be solved to obtain the value of $\cos\Phi$ by adding up the components along the principal diagonal of the matrices:

$$3\cos\Phi + (1-\cos\Phi)trace(nn^T) = trace\left(\frac{1}{2}(R+R^T)\right) \tag{33}$$

From equation (25), we get $trace(nn^T) = n^T n = 1$

$$\cos\Phi = \frac{1}{2}(R_{11}-R_{22}+R_{33}-1) \tag{34}$$

The angle Φ can be calculated from equation (32) or (34). For numerical reasons it is preferred to use equation (32) if $\sin\Phi \leq \frac{1}{2}\sqrt{2}$ and equation (34) if $\sin\Phi \geq \frac{1}{2}\sqrt{2}$.

As soon as $\sin\Phi$ is known, the value of n can be calculated from equation (31) if $\sin\Phi \neq 0$. From a numerical point of view this is not recommendable if the value of Φ approaches π radians. If the value of $\Phi > \frac{3}{4}\pi$ and we know the value of $\cos\Phi$, then equation (30) can be used to determine the value of n.

While:

$$(1-\cos\Phi)nn^T = \frac{1}{2}\left(R+R^T\right)-\cos\Phi I = [b_1 \quad b_2 \quad b_3 \quad] \tag{35}$$

It is seen that each of the columns b_1, b_2 and b_3 of the matrix $\frac{1}{2}\left(R+R^T\right)-\cos\Phi I$ is a vector in the same direction of n. So, apart from a factor, n is equal to b_1, b_2 and b_3.

Let b_i (i =1, 2 or 3) be the column with the greatest length $\sqrt{b_i^T b_i}$. Then the value of n is determined by:

$$b_i^T b_i = \max(b_1^T b_1, b_2^T b_2, b_3^T b_3);$$

$$n = \pm\frac{b_i}{\sqrt{b_i^T b_i}} \tag{36}$$

The sign of n must be selected such that $\sin\Phi$ in equation (31) is positive.

The translation t along the helical axis and the radius vector s of a point on this axis is obtained by solving the equations (25) and (27):

$$t = n^T v \tag{37}$$

$$s = -\frac{1}{2}n*(n*v)+\frac{\sin\Phi}{2(1-\cos\Phi)}n*v \tag{38}$$

The equations (36), (37), and (38) are true if and only if $\Phi \neq 0$. If $\Phi = 0$, then there is no rotation at all. In such a case the helical axis is not defined and the values of t, n and s are not unique. If $\Phi = 0$ and $v \neq 0$, then:

$$t = \sqrt{v^T v}$$

$$n = \frac{1}{t} v \qquad (39)$$

$$s = 0$$

As mentioned above, if $\Phi = 0$ and $v = 0$ there is no movement at all.

Chapter 4

Results And Discussion

This chapter explains in detail the verification of the least square minimization technique for determining the kinematic rigid body parameters. The accuracy of the Visual 3D software is substantiated using programs developed in MATLAB, version 7.0. As mentioned before, the biomechanical parameters i.e. translation vector and rotational matrix are the basic steps to determine the rigid body motion. Based on the least square minimization approach devised by Spoor and Veldpaus, programs are written in MATLAB to calculate these two parameters which are attached in Appendix B.

4.1 Elbow location from upper arm markers

Four markers are placed on the upper arm of the subject. These four markers are placed strategically on the upper arm; an upper arm lower lateral marker ALL, an upper arm lower medial marker ALM, an upper arm upper lateral marker AUL and an upper arm upper medial marker AUM. As the arm moves, the location co-ordinates of these joint markers are obtained with respect to the defined reference frame. This recorded marker trajectory data is analyzed against the static calibration data of the respective markers to obtain the translation vector v_{UAE} and the rotation matrix T_{UAE}. As shown in

the MATLAB code in Appendix B.1, the first step is to calculate the translation vector and rotation matrix.

For the upper arm, elbow is used as the calibration point. Location co-ordinates obtained from the medial and lateral markers placed on the elbow are averaged, such that this averaged value of the elbow markers is used as the averaged elbow reference calibration point.

4.1.1. Movement Relative to Calibration Position

The trajectory of the elbow can be described by the movement of 2 different body segments: distal upper arm and the proximal forearm. The 3D software calculates the trajectory traced by the elbow. In order to verify the accuracy of the calculated elbow trajectory of the 3D program, we revise our approach. The averaged elbow calibration marker is utilized as the radius vector in position 1 to determine the radius vector in position 2, with the values of the translation vector v_{UAE} and rotation matrix T_{UAE} calculated from the four upper arm markers. This new radius vector in position 2 calculated with respect to the averaged elbow marker (defined as calibration point) in position 1 should be similar to the traced elbow trajectory determined by the 3D program in order to verify its correctness.

Figure 4.1, 4.2 and 4.3 show clearly the comparison between the Visual 3D elbow trajectory values and the calculated values with respect to the averaged elbow calibration marker along the X, Y and Z axes respectively for the upper arm movement. From the

graphs we find that there are variations between the pre determined and the calculated values.

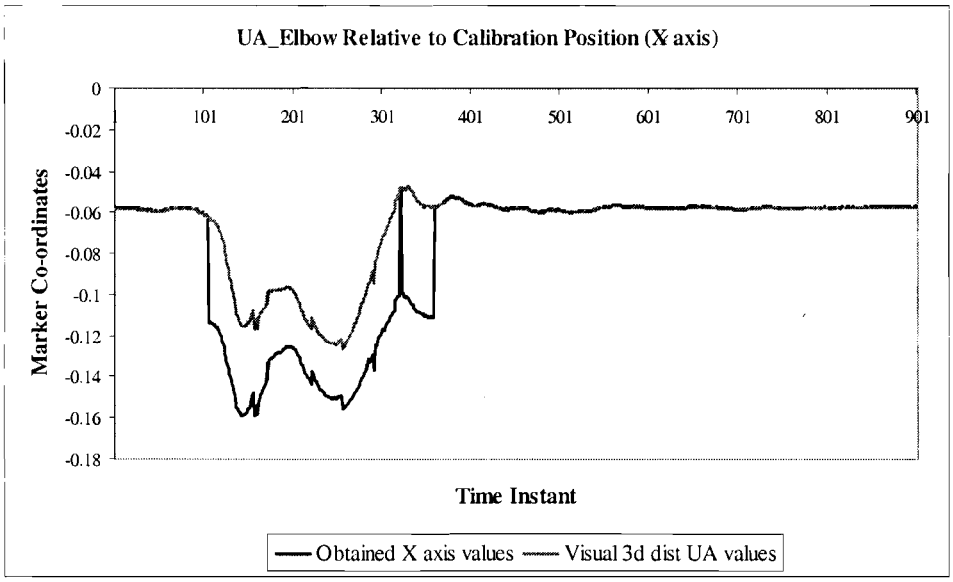

Figure 4.1 Elbow location from upper arm markers relative to the Calibration Position along the X axis

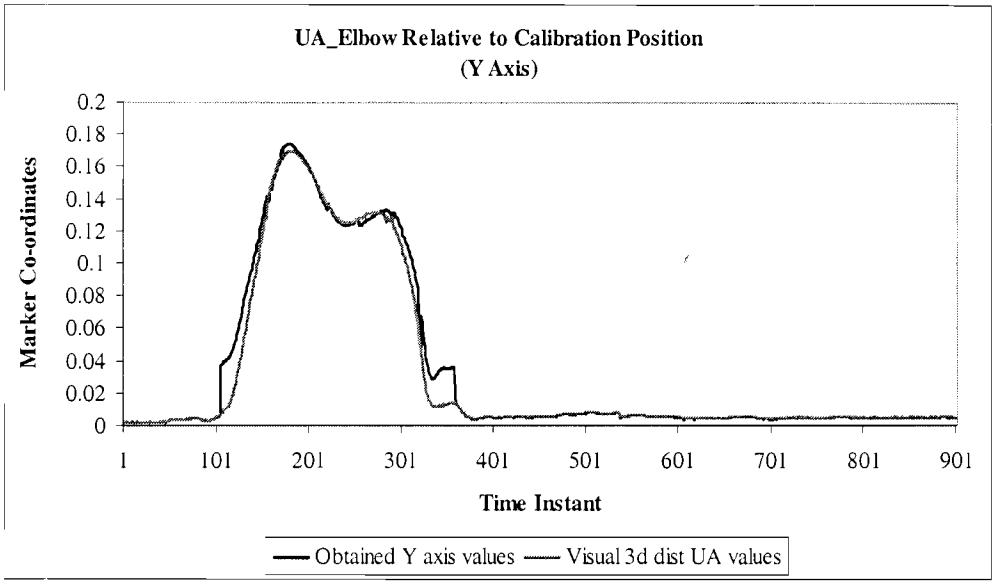

Figure 4.2 Elbow location from upper arm markers relative to the Calibration Position along the Y axis

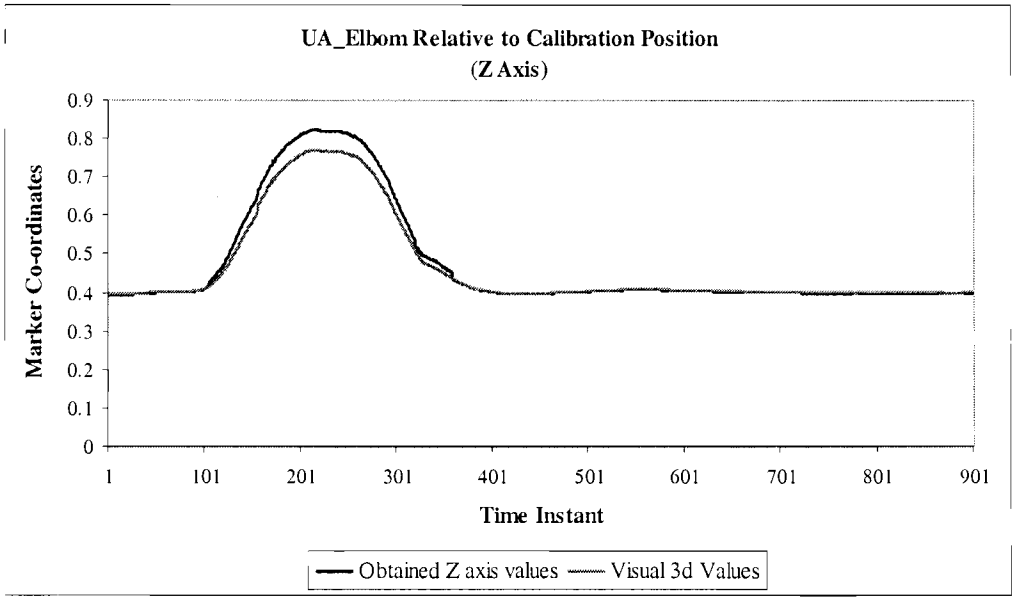

Figure 4.3 Elbow location from upper arm markers relative to the Calibration Position along the Z axis

4.1.2 Movement Relative to Previous Position

The previous calculation for the position 2 radius vector of the elbow was done with reference to the elbow as the calibration position. However, if this method is modified to include the every recorded previous positions, to determine the next location, the output varies. As mentioned if the radius vector of the elbow in position 2 is calculated with respect to the radius vector in position 1 at the first step and thereafter it is calculated with respect to the previous detected vector at each location, then the output is found to produce oscillations.

Figure 4.4, 4.5 and 4.6 show clearly the comparison between the Visual 3D elbow trajectory values and the calculated values with respect to the averaged elbow calibration at the first step and thereafter with respect to the previous position along the X, Y and Z axes respectively.

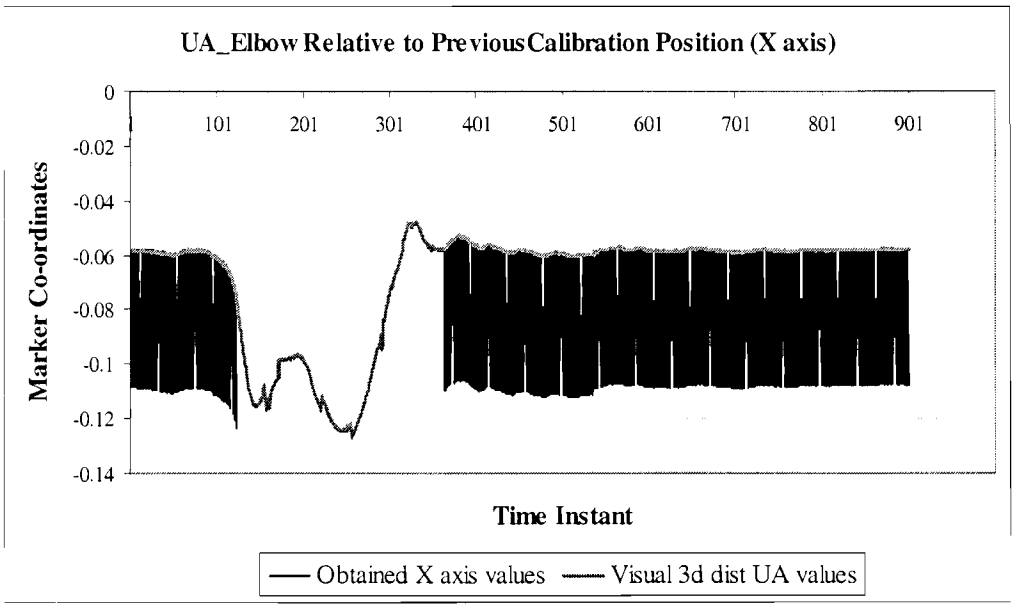

Figure 4.4 Elbow location from upper arm markers relative to the Previous Position along the X axis

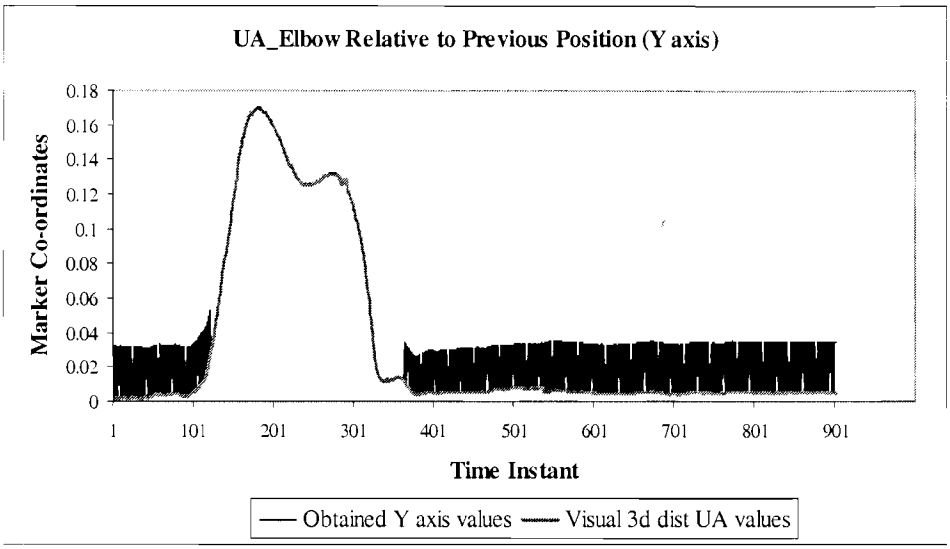

Figure 4.5. Elbow location from upper arm markers relative to the Previous Position along the Y axis

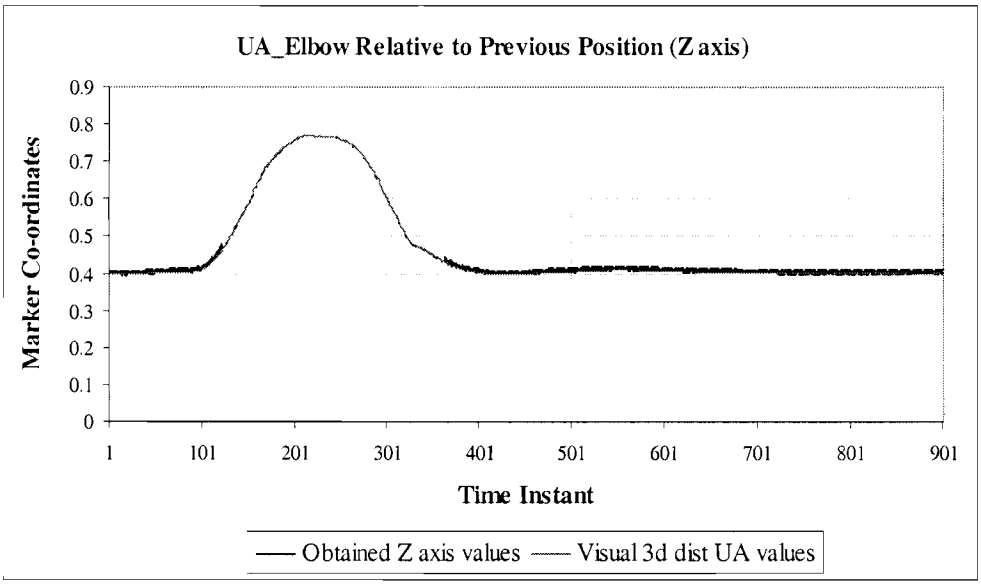

Figure 4.6. Elbow location from upper arm markers relative to the Previous Position along the Z axis

4.1.2.1 Relative to Previous Position with Identity Rotation Compensation

From the output of the program in Appendix B.2 and the Figures 4.4, 4.5 and 4.6, we see that the translation vector is nearing zero when the arm is in motion. However it is high when the arm is stationary resulting in oscillations. This could be because the elbow co-ordinates in position 2 are calculated with respect to the previous position. By calculating the new position with respect to an identity rotation matrix, instead of the rotation at the previous position every time the translation vector is high reduces the oscillations along the X, Y and Z axes respectively as shown in Figure 4.7, 4.8 and 4.9.

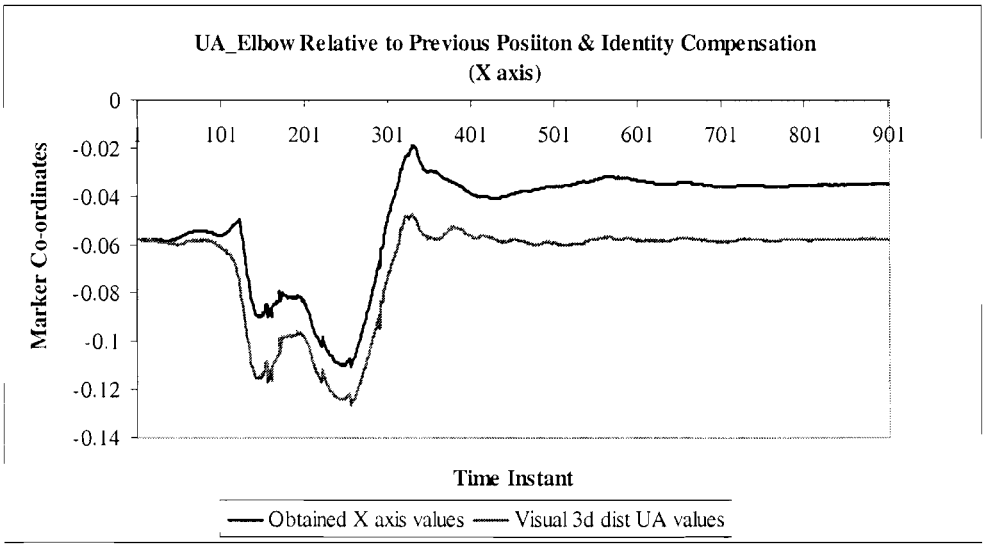

Figure 4.7. Elbow location from upper arm markers relative to the Previous Position and an Identity Rotation Compensation along the X axis

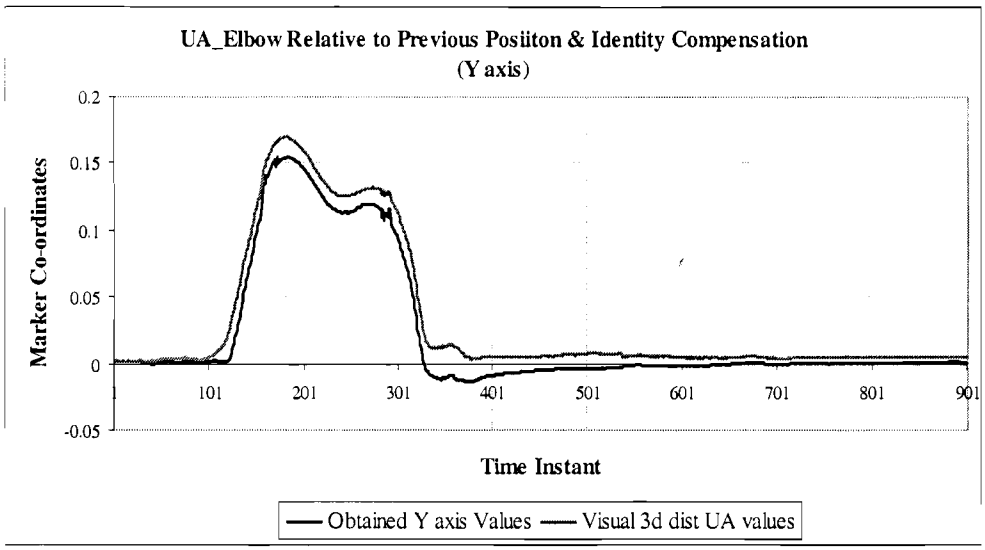

Figure 4.8. Elbow location from upper arm markers relative to the Previous Position and an Identity Rotation Compensation along the Y axis

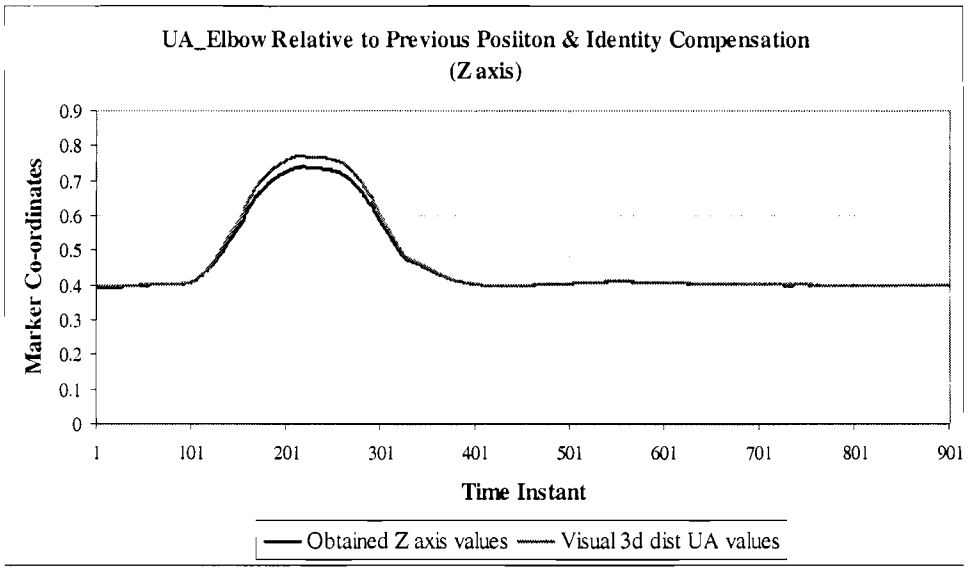

Figure 4.9. Elbow location from upper arm markers relative to the Previous Position and an Identity Rotation Compensation along the Z axis

4.1.2.2 Relative to Previous Position with Averaging Compensation

From the output of the program attached in Appendix B.2 and the Figures 4.4, 4.5 and 4.6, we see that the obtained elbow trajectory values oscillate back and forth alternately when the arm is stationary. The obtained elbow co-ordinates are double the actual value because of these oscillations, with the swinging being more evident along the movement in the X-axis. This could be because the elbow co-ordinates in position 2 are calculated with respect to the previous position. An averaging compensation provided between two oscillations nullifies the oscillation effect, as shown in the output of Appendix B.4 and Figures 4.10, 4.11 and 4.12.

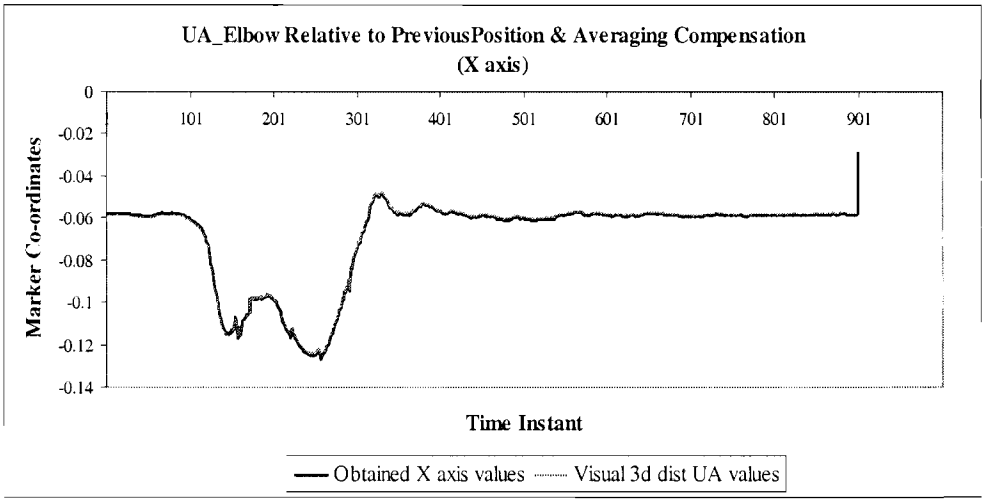

Figure 4.10. Elbow location from upper arm markers relative to the Previous Position and Averaging Compensation along the X axis

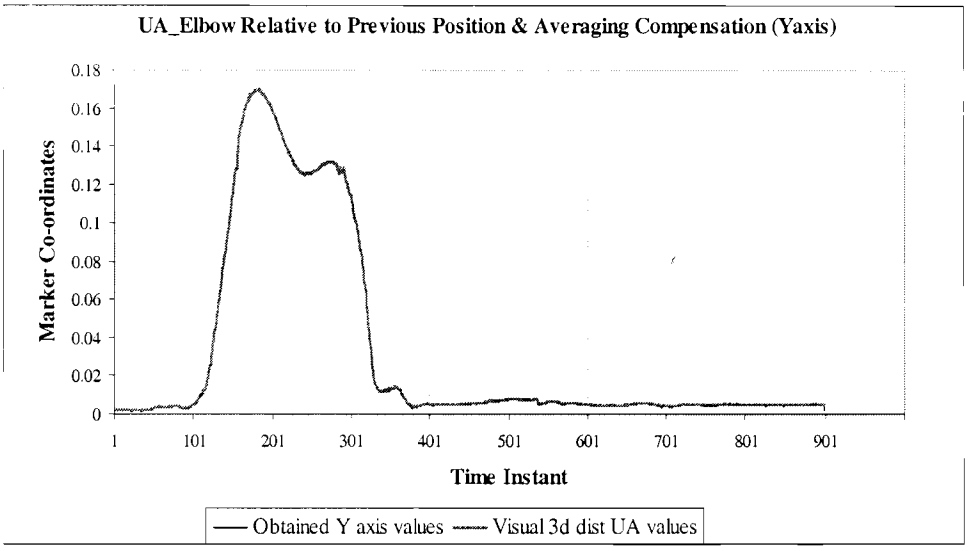

Figure 4.11. Elbow location from upper arm markers relative to the Previous Position and Averaging Compensation along the Y axis

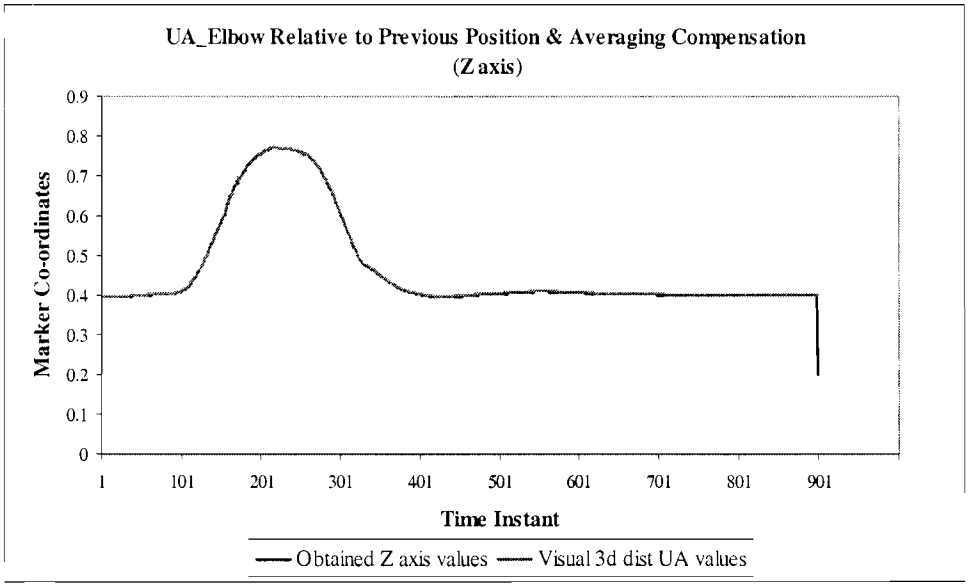

Figure 4.12. Elbow location from upper arm markers relative to the Previous Position and Averaging Compensation along the Z axis

4.2 Elbow location from forearm markers

Four markers are placed on the forearm of the subject. These four markers are placed strategically on the forearm; a forearm lower lateral marker FLL, a forearm lower medial marker FLM, a forearm upper lateral marker FUL, and a forearm upper medial marker FUM. As the arm moves, the location co-ordinates of these joint markers are obtained with respect to the reference frame defined. This recorded marker trajectory data is analyzed against the static calibration data of the respective markers to obtain the translation vector v_{FAE} and the rotation matrix T_{FAE}. As shown in the MATLAB code in Appendix B.5, the first step is to calculate the translation vector and rotation matrix.

For the forearm, both the elbow and the wrist are used as calibration points depending on the trial. Location co-ordinates obtained from the medial and lateral markers placed on the elbow are averaged, such that this averaged value of the elbow markers is used as the reference calibration point in the 1st trial.

4.2.1. Movement Relative to Calibration Position

The trajectory of the elbow can be described by the movement of 2 different body segments: distal upper arm and the proximal forearm. The 3D software calculates the trajectory traced by the elbow. In order to verify the accuracy of the calculated elbow trajectory of the 3D program, we revise our approach. The averaged elbow calibration marker is utilized as the radius vector in position 1 to determine the radius vector in position 2, with the values of the translation vector v_{FAE} and rotation matrix T_{FAE}

calculated from the four forearm markers. This new radius vector in position 2 calculated with respect to the averaged elbow marker (defined as calibration point) in position 1 should be similar to the traced elbow trajectory determined by the 3D program.

Figure 4.13, 4.14 and 4.15 show clearly the comparison between the Visual 3D elbow trajectory values and the calculated values with respect to the averaged elbow calibration marker along the X, Y and Z axes respectively for the forearm movement. From the graphs we find that there are variations between the pre determined experimental and the calculated values.

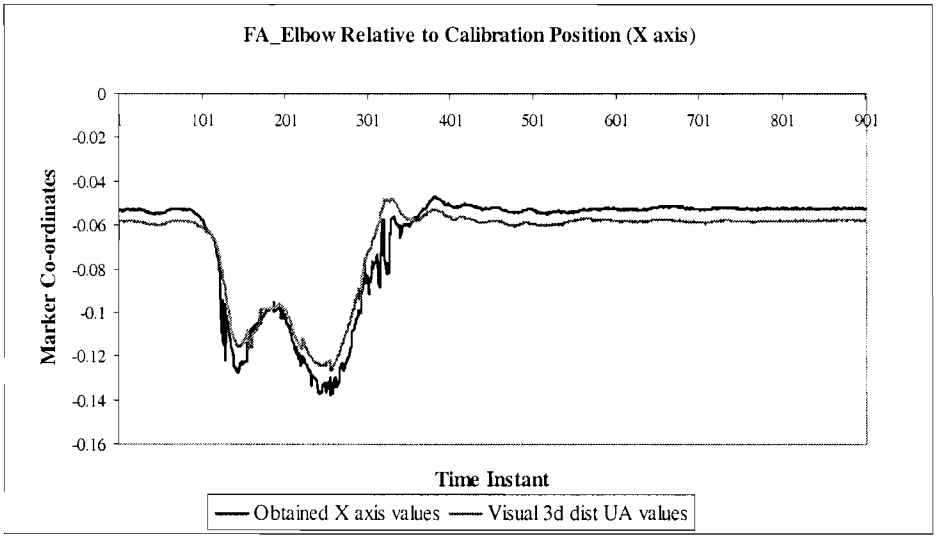

Figure 4.13 Elbow location from forearm markers relative to the Calibration Position along the X axis

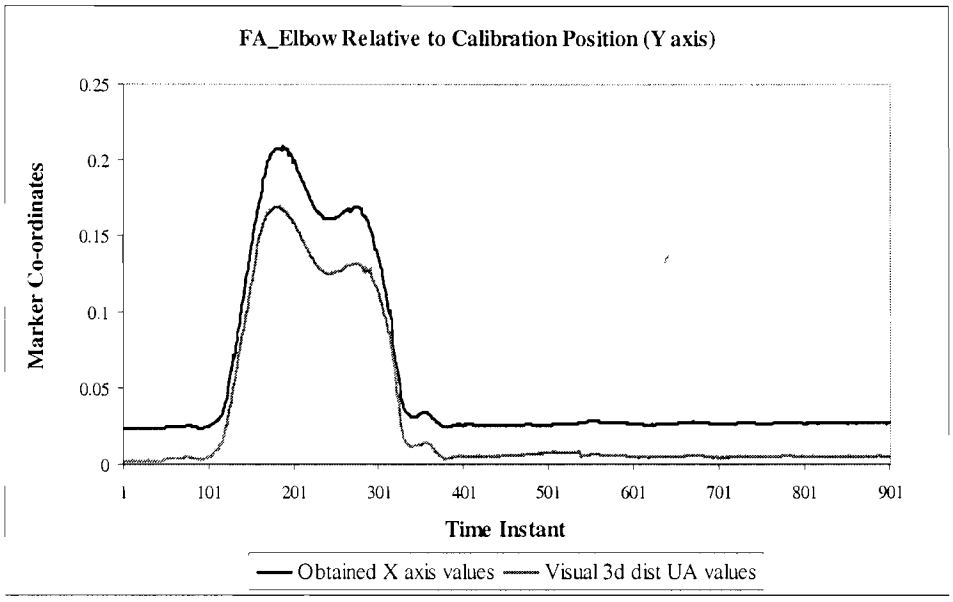

Figure 4.14 Elbow location from forearm markers relative to the Calibration Position along the Y axis

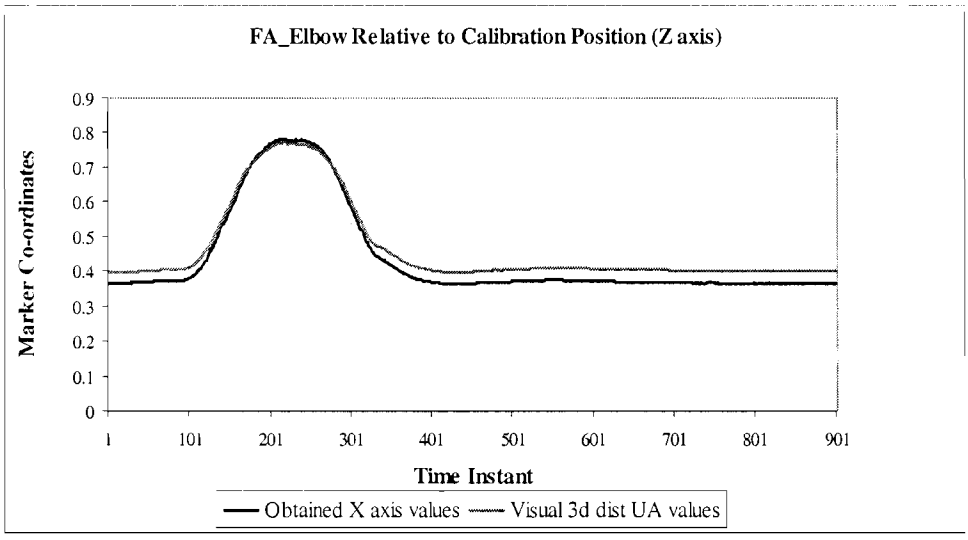

Figure 4.15 Elbow location from forearm markers relative to the Calibration Position along the Z axis

4.2.2 Movement Relative to Previous Position

The above calculation for the position 2 radius vector of the elbow was done with reference to the calibration position of the elbow. However if this is modified to include the every recorded previous position to determine the next location, the output varies. As mentioned, if the radius vector of the elbow in position 2 is calculated with respect to the radius vector in position 1 at the first step and thereafter it is calculated with respect to the respect to the previous detected vector at each location, then the output is found to produce oscillations as shown below.

Figure 4.16, 4.17 and 4.18 shows clearly the comparison between the Visual 3D elbow trajectory values and the calculated values with respect to the averaged elbow calibration at the first step and thereafter with respect to the previous position along the X, Y and Z axes respectively for the forearm.

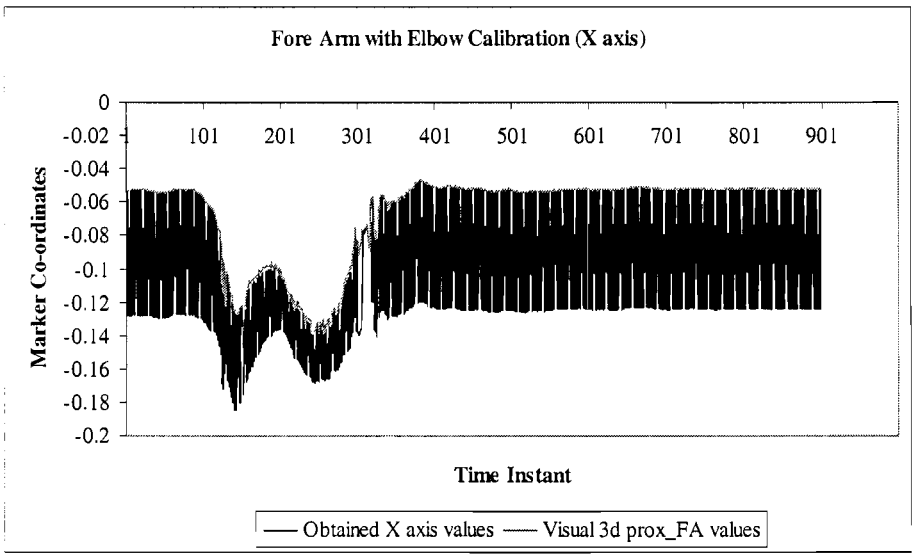

Figure 4.16. Elbow location from forearm markers relative to the Previous Position along the X axis

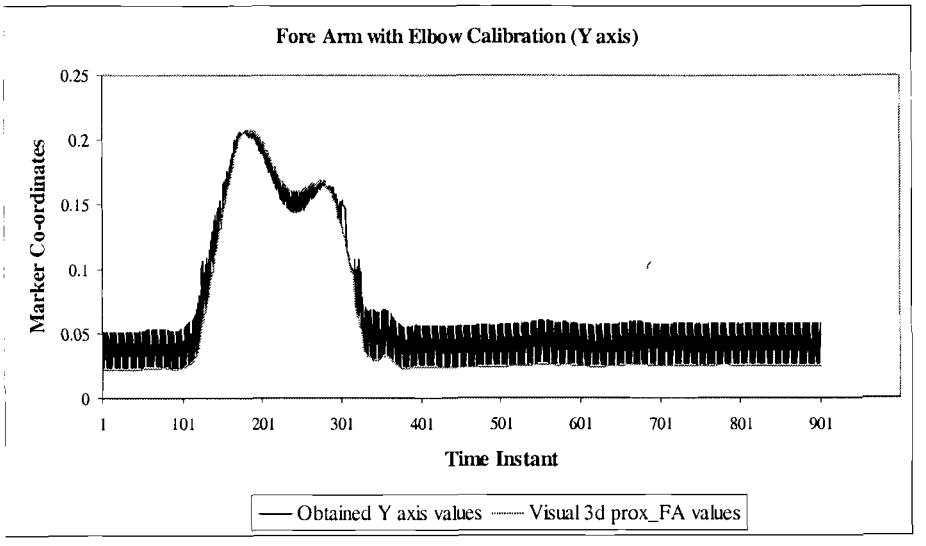

Figure 4.17. Elbow location from forearm markers relative to the Previous Position along the Y axis

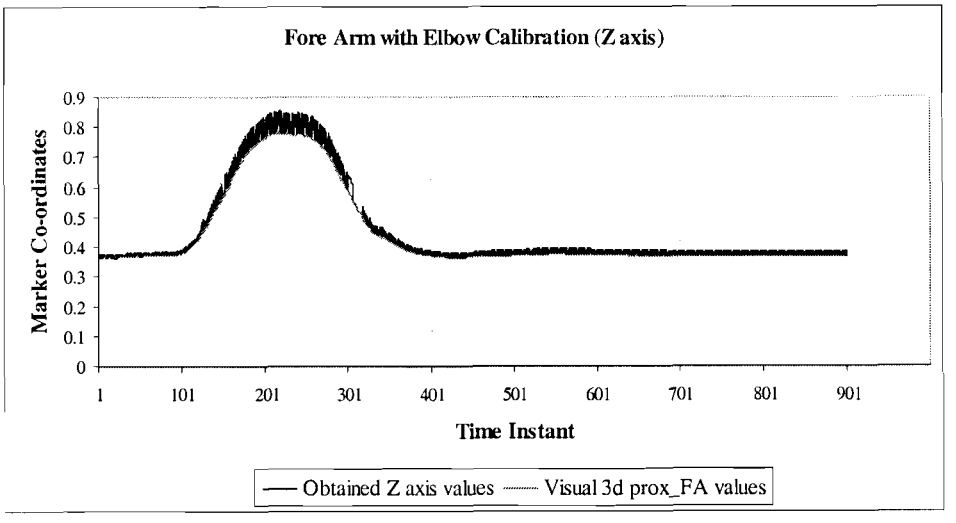

Figure 4.18. Elbow location from forearm markers relative to the Previous Position along the Z axis

4.2.2.1 Relative to Previous Position with Identity Rotation Compensation

From the output pf the program attached in Appendix B.6 and the Figures 4.16, 4.17 and 4.18, we see that the translation vector is nearing zero when the arm is in

motion. However it is high when the arm is moving resulting in more oscillations during motion which is more evident along the X-axis. This is because the elbow co-ordinates in position 2 are calculated with respect to the previous position. By calculating the new position with respect to an identity rotation matrix, instead of the rotation at the previous position every time the translation vector is high, reduces the oscillations to some extent along the X, Y and Z axes respectively as shown in Figure 4.19, 4.20 and 4.21.

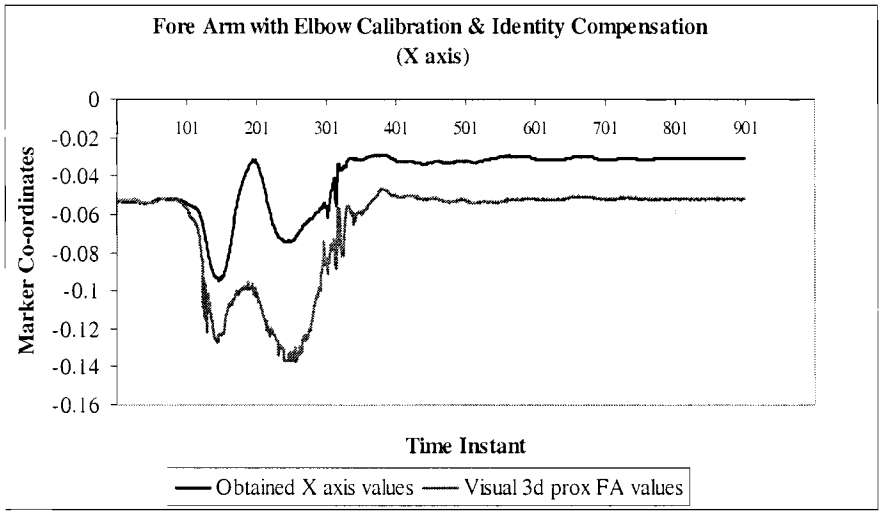

Figure 4.19. Elbow location from forearm markers relative to the Previous Position and an Identity Rotation Compensation along the X axis

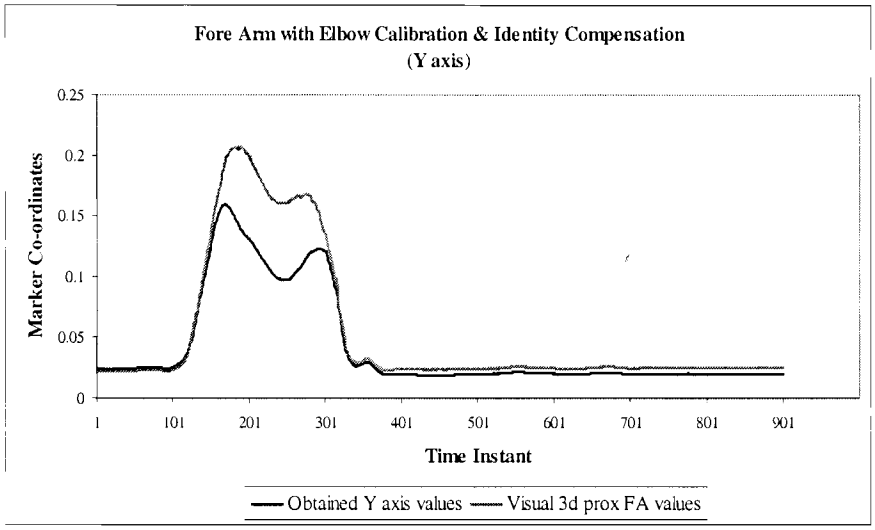

Figure 4.20. Elbow location from forearm markers relative to the Previous Position and an Identity Rotation Compensation along the Y axis

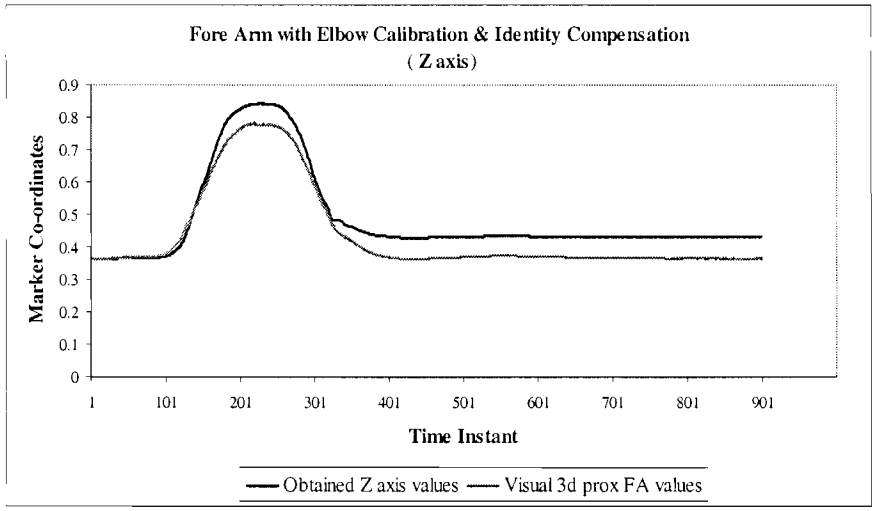

Figure 4.21. Elbow location from forearm markers relative to the Previous Position and an Identity Rotation Compensation along the Z axis.

4.2.2.2 Relative to Previous Position with Averaging Compensation

From the output attached in Appendix B.6 and the Figures 4.16, 4.17 and 4.18, we see that the obtained elbow trajectory values oscillate back and forth alternately when the

arm is in motion. The obtained elbow co-ordinates are double the actual value because of these oscillations, with the swinging being more evident along the movement in the X-axis. This is because the elbow co-ordinates in position 2 are calculated with respect to the previous position. An averaging compensation provided at each oscillation nullifies the oscillation effect which can be seen clearly from the output of the program in Figures 4.21, 4.22 and 4.23.

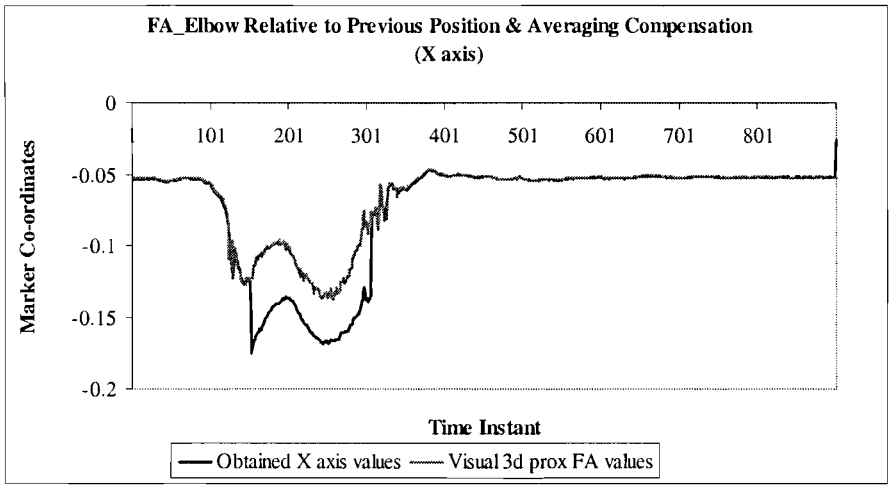

Figure 4.22. Elbow location from forearm markers relative to the Previous Position and Averaging Compensation along the X axis

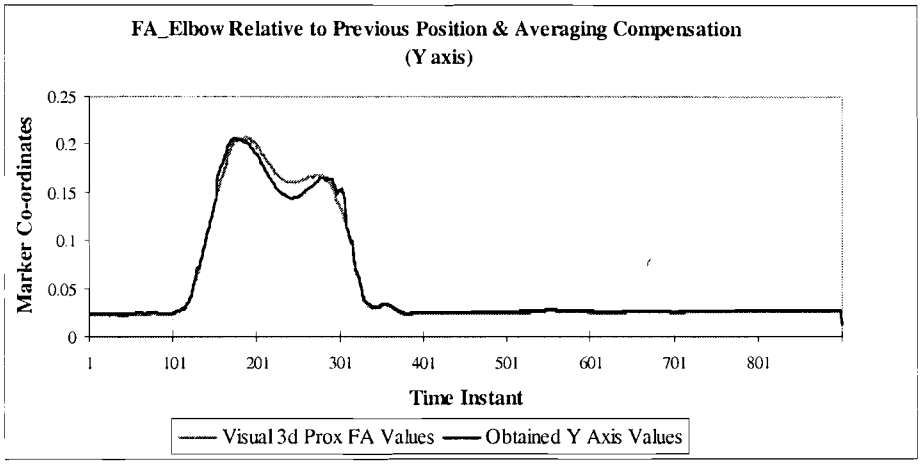

Figure 4.23. Elbow location from forearm markers relative to the Previous Position and Averaging Compensation along the Y axis

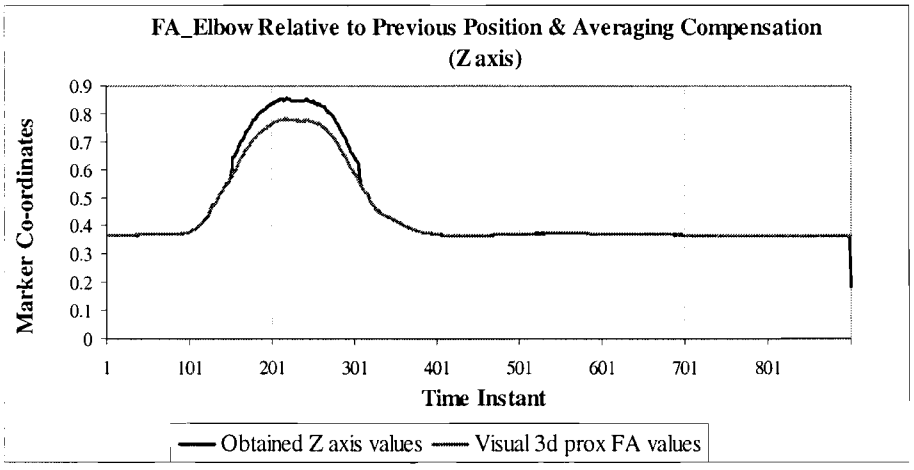

Figure 4.24. Elbow location from forearm markers relative to the Previous Position and Averaging Compensation along the Z axis

4.3. Wrist location from forearm markers

The four markers placed on the forearm of the subject for testing with respect to the wrist as the joint center of motion are similar to the ones used in previous trial with respect to elbow viz. FLL, FLM, FUL, and FUM. The location co-ordinates obtained

from the medial and lateral markers placed on the wrist is averaged, such that this averaged value of the wrist markers is used as the reference calibration point.

4.3.1. Movement Relative to Calibration Position

The trajectory of the wrist can be described by the movement of 2 different body segments: proximal forearm and the hand. The 3D software calculates the trajectory traced by the wrist. In order to verify the accuracy of the calculated wrist trajectory of the 3D program, we revise our approach. The averaged wrist calibration marker is utilized as the radius vector in position 1 to determine the radius vector in position 2, with the values of the translation vector v_{FAW} and rotation matrix T_{FAW} calculated from the four forearm markers. This new radius vector in position 2 calculated with respect to the averaged wrist marker (defined as calibration point) in position 1 should be similar to the traced wrist trajectory determined by the 3D program.

Figure 4.25, 4.26 and 4.27 show clearly the comparison between the Visual 3D wrist trajectory values and the calculated values with respect to the averaged wrist calibration marker along the X, Y and Z axes respectively for the forearm movement. From the graphs we find that there are negligible variations between the experimental and the calculated values.

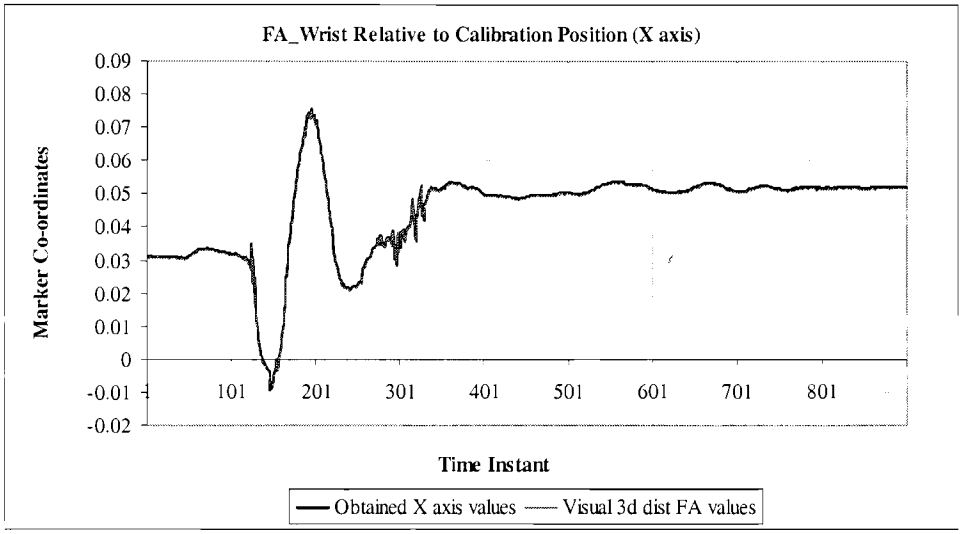

Figure 4.25 Wrist location from forearm markers relative to the Calibration Position along the X axis.

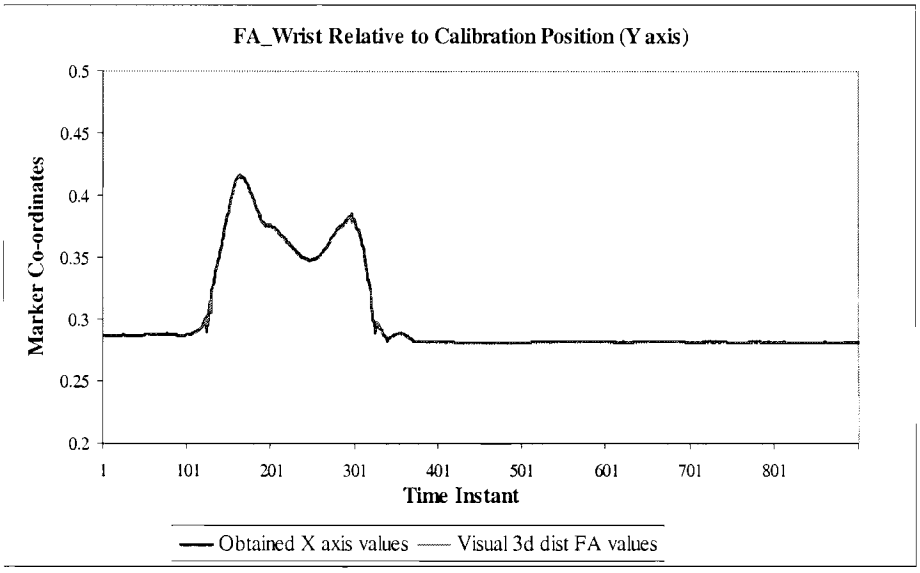

Figure 4.26 Wrist location from forearm markers relative to the Calibration Position along the Y axis.

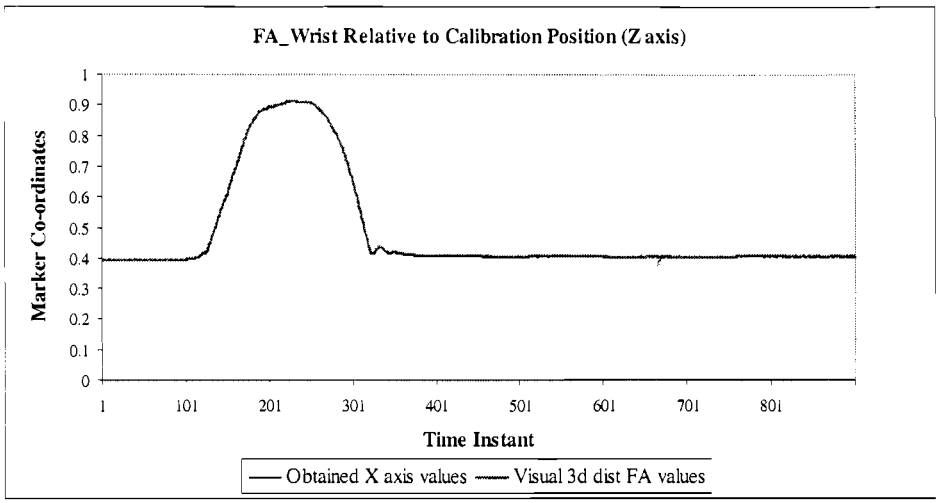

Figure 4.27 Wrist location from forearm markers relative to the Calibration Position along the Z axis.

4.3.2 Movement Relative to Previous Position

The above calculation for the position 2 radius vector of the wrist was done with reference to the calibration position of the wrist. However if this is modified to include the recorded previous positions to determine the next location, the output varies. As mentioned if the radius vector of the wrist in position 2 is calculated with respect to the radius vector in position 1 at the first step and thereafter it is calculated with respect to the respect to the previous detected vector at each location, then the output is found to produce oscillations as shown below.

Figure 4.28, 4.29 and 4.30 shows clearly the comparison between the Visual 3D wrist trajectory values and the calculated values with respect to the averaged wrist calibration at the first step and thereafter with respect to the previous position along the X, Y and Z axes respectively for the forearm.

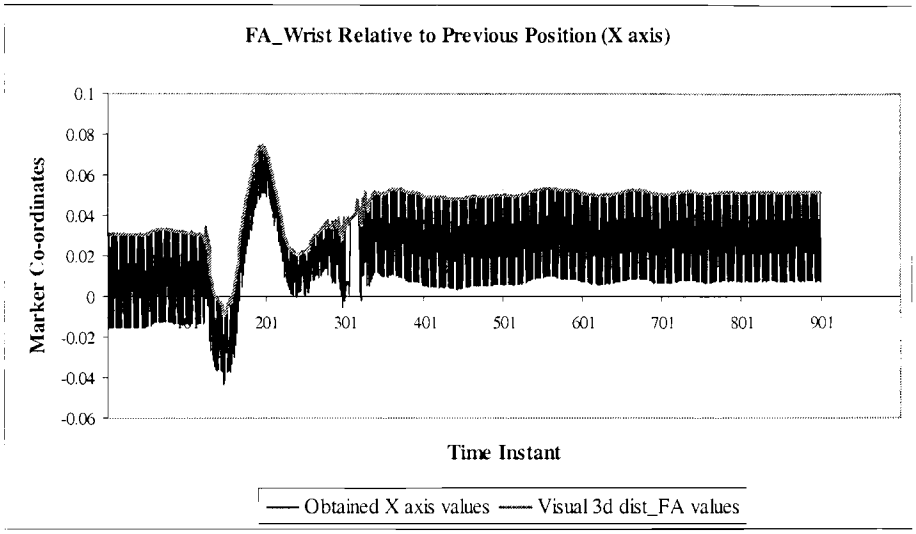

Figure 4.28 Wrist location from forearm markers relative to the Previous Position along the X axis.

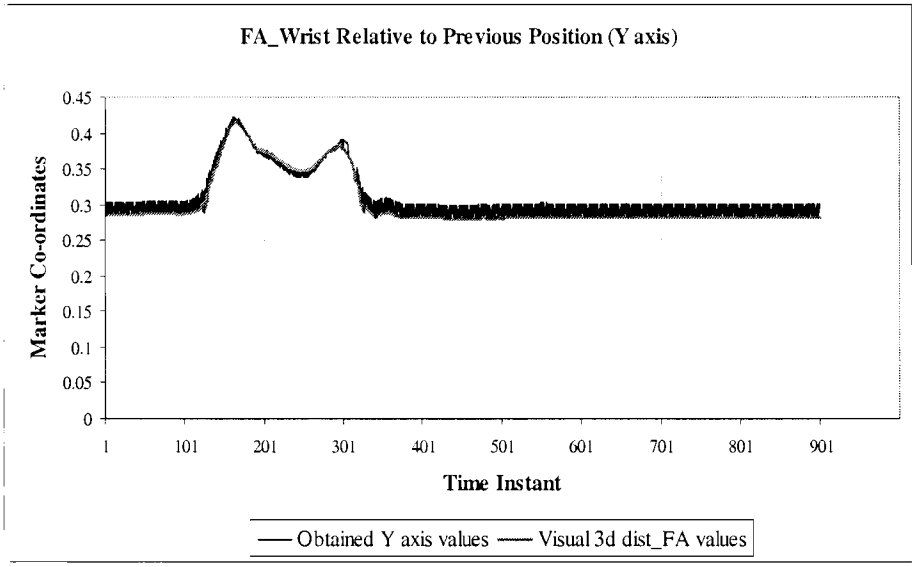

Figure 4.29 Wrist location from forearm markers relative to the Previous Position along the Y axis.

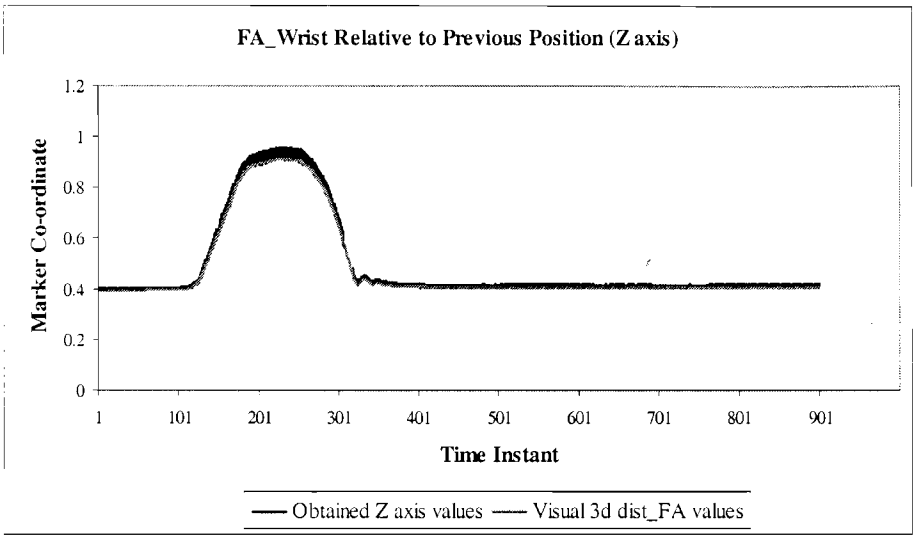

Figure 4.30 Wrist location from forearm markers relative to the Previous Position along the Z axis.

4.3.2.1 Relative to Previous Position with Identity Rotation Compensation

From the output of the program attached in Appendix B.10 and the Figures 4.28, 4.29 and 4.30, we see that the translation vector is high when the arm is in motion, resulting in more oscillations during motion which is more evident along the X-axis. This could be because the wrist co-ordinates in position 2 are calculated with respect to the previous position. By calculating the new position with respect to an identity rotation matrix, instead of the rotation at the previous position every time the translation vector is high, reduces the oscillations to some extent along the X, Y and Z axes respectively as shown in Figure 4.31, 4.32 and 4.33.

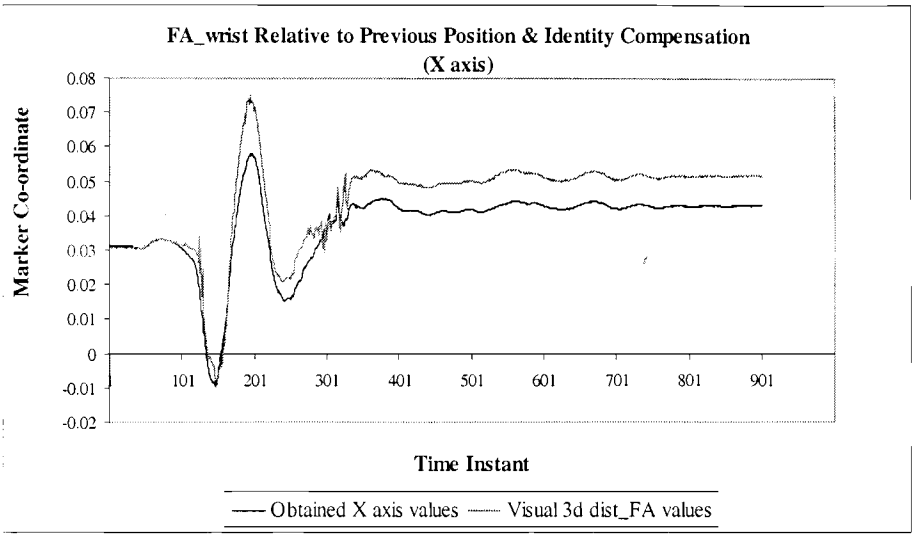

Figure 4.31 Wrist location from forearm markers relative to the Previous Position and an Identity Rotation Compensation along the X axis.

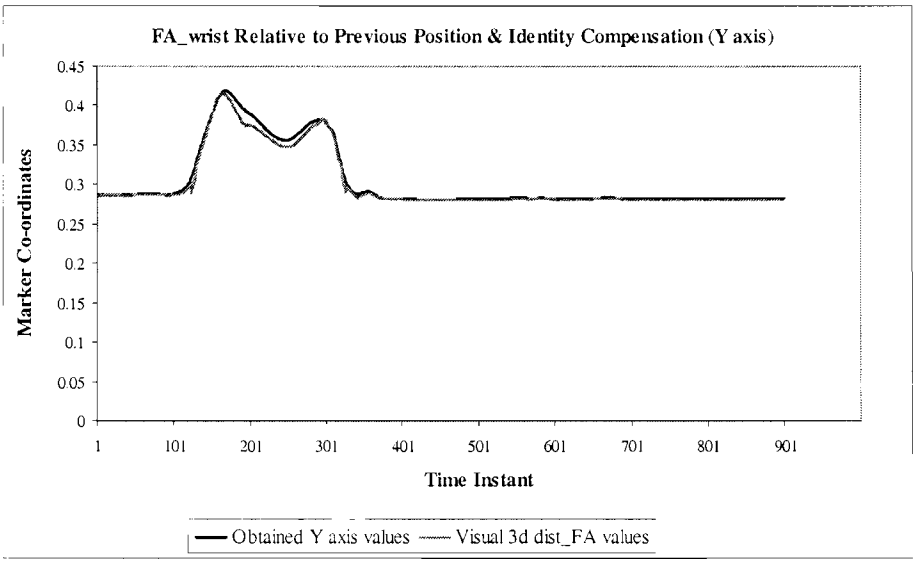

Figure 4.32 Wrist location from forearm markers relative to the Previous Position and an Identity Rotation Compensation along the Y axis.

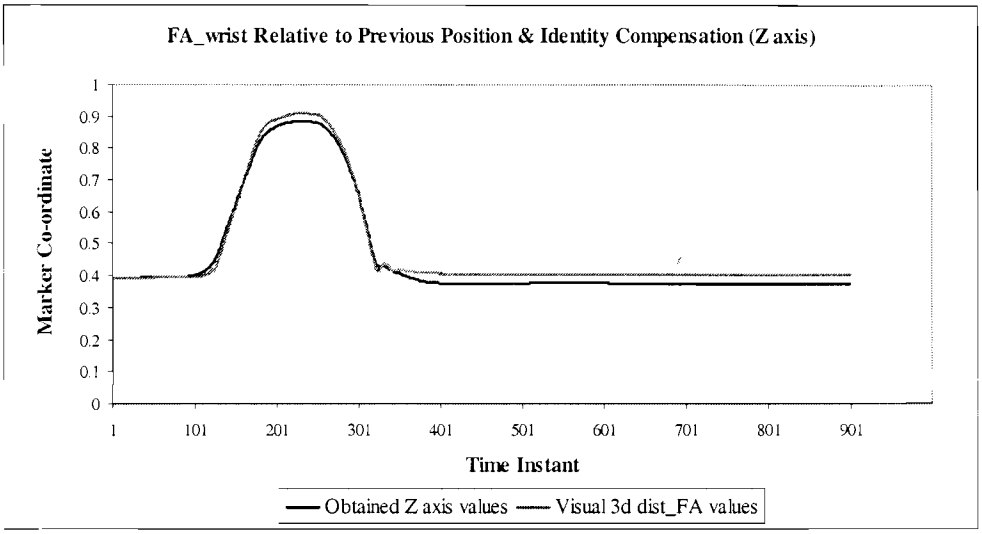

Figure 4.33 Wrist location from forearm markers relative to the Previous Position and an Identity Rotation Compensation along the Z axis.

4.3.2.2 Relative to Previous Position with Averaging Compensation

From the output of the program attached in Appendix B.10 and the Figures 4.28, 4.29 and 4.30, we see that the obtained wrist trajectory values oscillate back and forth alternately when the arm is in motion. The obtained wrist co-ordinates are double the actual value because of these oscillations, with the swinging being more evident along the movement in the X-axis. This is because the wrist co-ordinates in position 2 are calculated with respect to the previous position. An averaging compensation provided at each oscillation nullifies the oscillation effect as shown in output attached in Figures 4.34, 4.35 and 4.36.

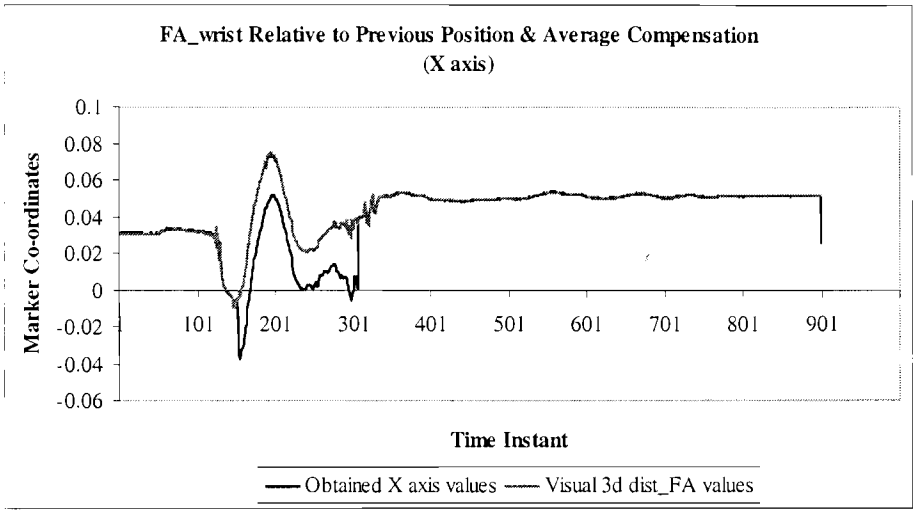

Figure 4.34 Wrist location from forearm markers relative to the Previous Position and an Averaging Compensation along the X axis.

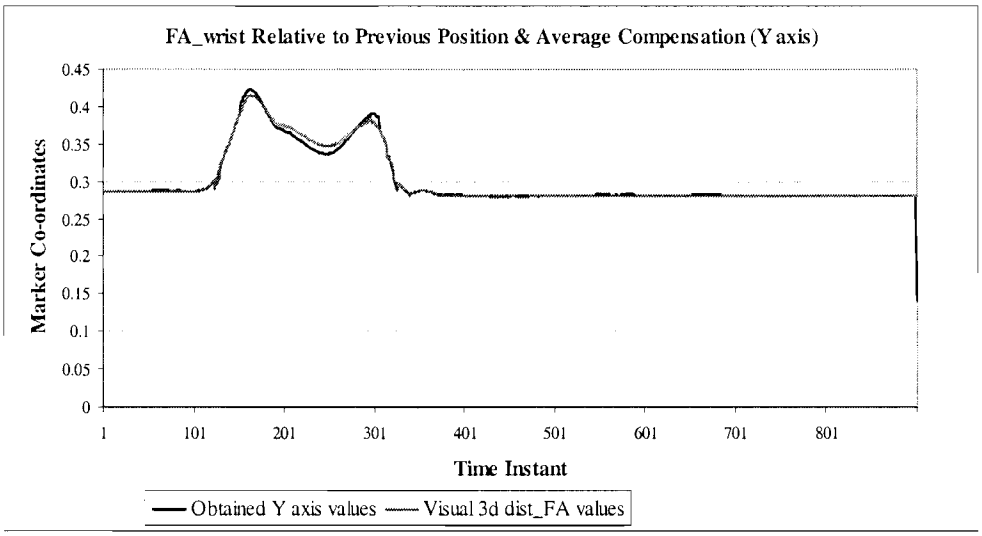

Figure 4.35 Wrist location from forearm markers relative to the Previous Position and an Averaging Compensation along the Y axis.

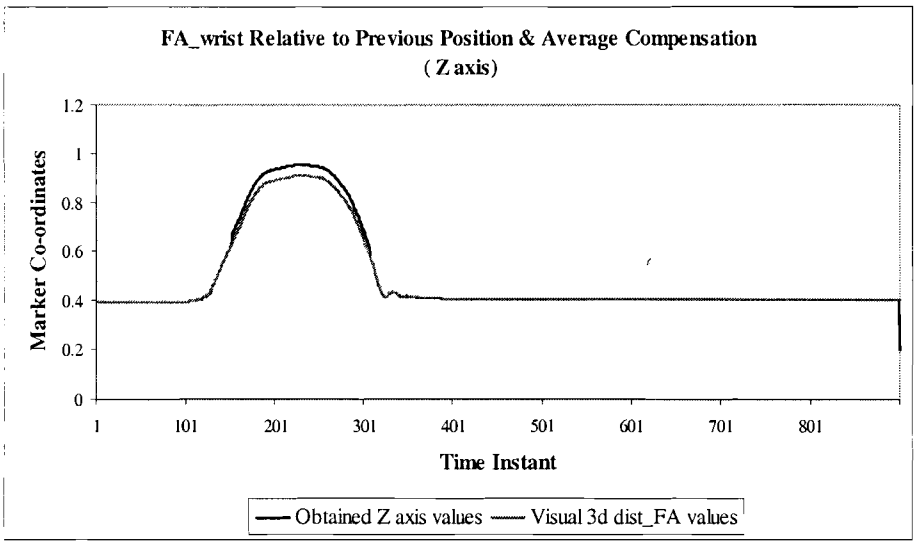

Figure 4.36 Wrist location from forearm markers relative to the Previous Position and an Averaging Compensation along the Z axis.

4.4. Three Marker Verification

A minimum of three non-collinear markers per segment are needed to measure the six degree of freedom to determine the rigid body motion. In order to substantiate the precision of the Visual 3D calculations, four markers were utilized each on the upper and the forearm for the above verifications. The generated code was found to correlate with the Visual 3D program generating identical results of the elbow trajectory. The accuracy of the program can be further verified by utilizing only the required minimum of only three markers.

4.4.1 Without Upper Arm Upper Medial Marker AUM

For the upper arm, the upper medial marker AUM is removed. Only the location co-ordinates of the remaining three markers AUL, ALL and ALM are recorded and

utilized as the input trajectory data. Similarly for the static reference frame, only the similar three markers are considered, excluding AUM and their locations determined for the static calibration reference input. The rotation matrix and the translation vector are computed; these kinematic parameters are of the AUM marker with respect to the other three markers. In order to verify the accuracy further, the three marker approach is tested relative to the assumed calibration position and the previous position of the marker.

4.4.1.1 Relative to Calibration Position

The AUM marker is utilized as the radius vector in position 1 to determine the radius vector in position 2, with the values of the translation vector and rotation matrix calculated from the three upper arm markers. This new radius vector in position 2 calculated with respect to the AUM calibration marker (defined as calibration point) in position 1 is found to be similar to the traced AUM marker trajectory obtained from the data acquisition system.

Figure 4.37, 4.38 and 4.39 show clearly the comparison between the traced AUM marker trajectory values and the calculated values, along the X, Y and Z axes respectively for the upper arm movement. From the graphs we find that there is negligible variation between the traced AUM marker values and the calculated values.

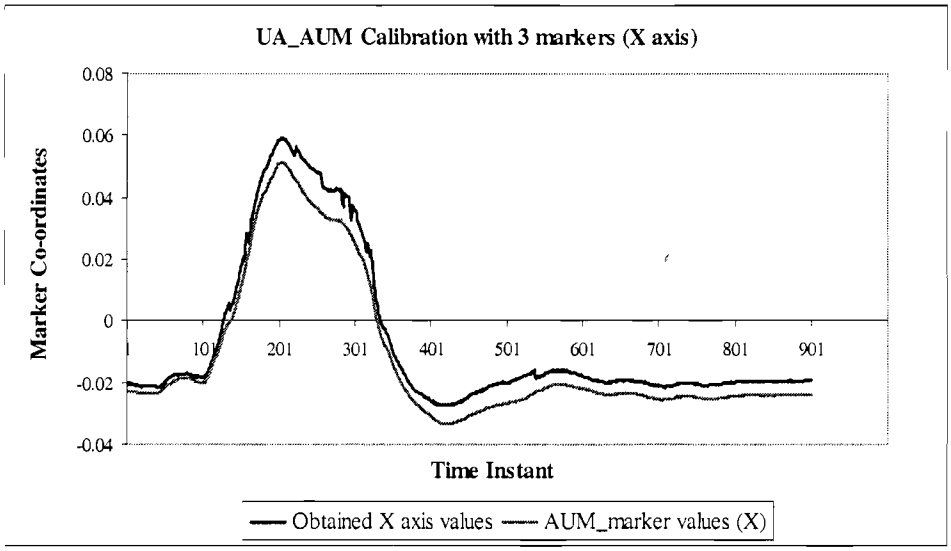

Figure 4.37 Comparison of traced AUM marker X-axis values and determined X-axis values relative to the calibration position for the upper arm.

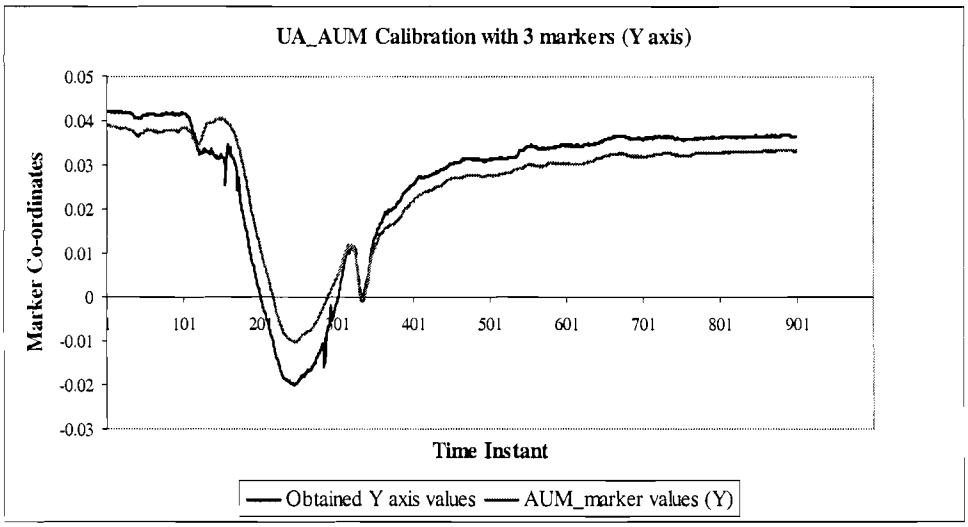

Figure 4.38 Comparison of traced AUM marker Y-axis values and determined Y-axis values relative to the calibration position for the upper arm.

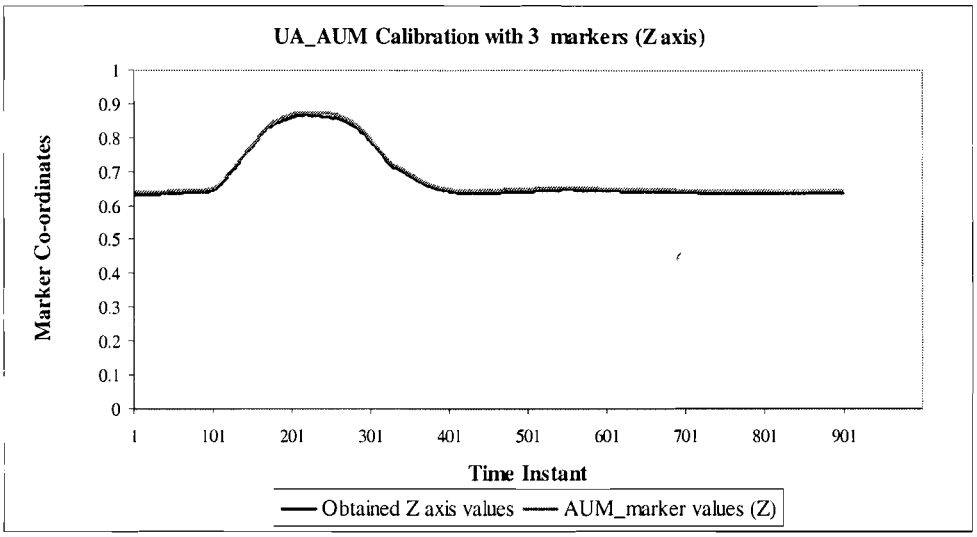

Figure 4.39 Comparison of traced AUM marker Z-axis values and determined Z-axis values relative to the calibration position for the upper arm.

4.4.1.2 Relative to Previous Position with Averaging Compensation

On implementing this same approach of utilizing three markers and determining the trajectory, relative to the previous position with averaging compensation, it is found that the calculated values follow the same trajectory pattern as the pre-determined AUM marker. This is shown in figures 4.40, 4.41 and 4.42.

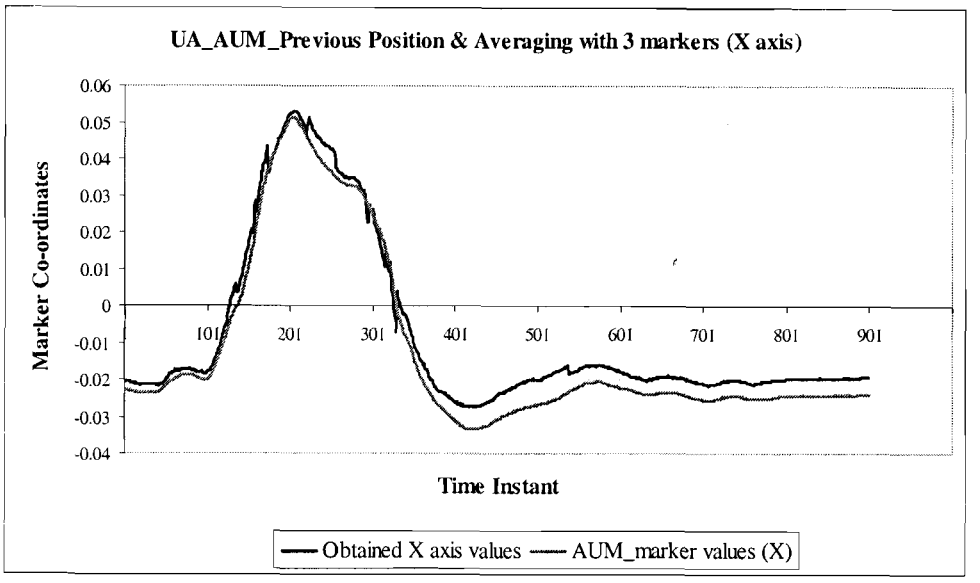

Figure 4.40 Comparison of traced AUM marker X-axis values and determined X-axis values relative to the previous position with averaging compensation for the upper arm.

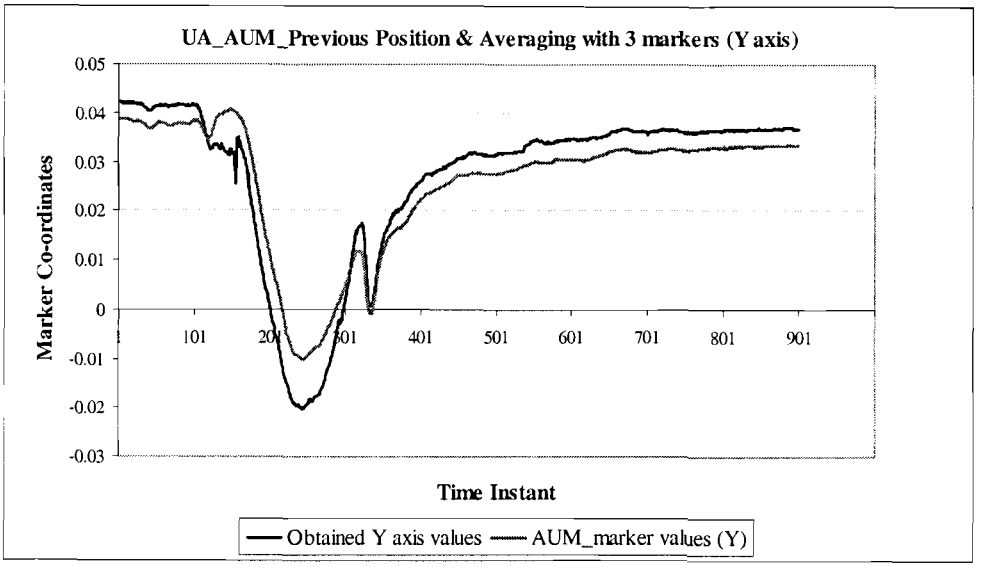

Figure 4.41 Comparison of traced AUM marker Y-axis values and determined Y-axis values relative to the previous position with averaging compensation for the upper arm.

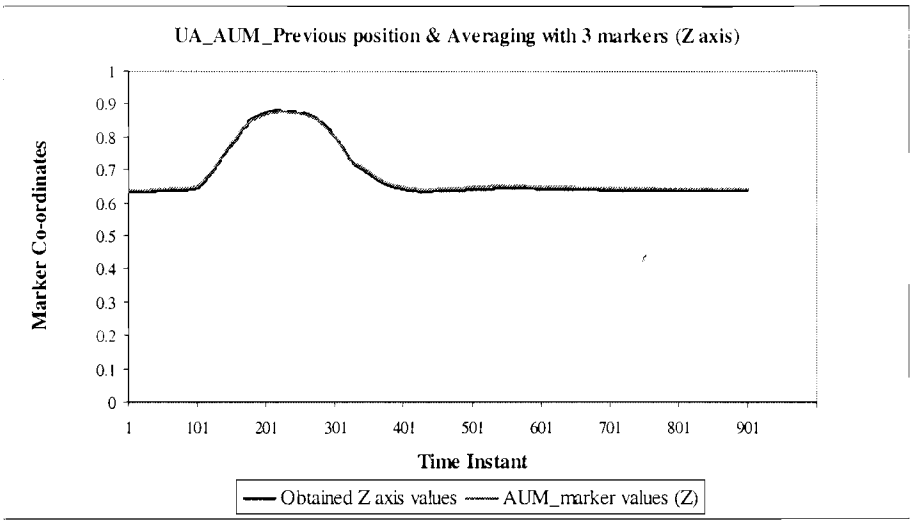

Figure 4.42 Comparison of traced AUM marker Z-axis values and determined Z-axis values relative to the previous position with averaging compensation for the upper arm.

4.4.2 Without Forearm Upper Medial Marker FUM

For the forearm, the upper medial marker FUM is removed. Only the location co-ordinates of the remaining three markers FUL, FLL and FLM are recorded and utilized as the input trajectory data. Similarly for the static reference frame, only the similar three markers are considered, excluding FUM and their locations determined for the static calibration reference input. The calibration position of the excluded fourth marker FUM is considered as the reference calibration point to compute the rotation matrix and the translation vector. These computed kinematic parameters are of the FUM marker with respect to the other three markers. In order to verify the accuracy further, the three marker approach is tested relative to the assumed calibration position and the previous position of the marker.

4.4.2.1 Relative to Calibration Position

The FUM marker is utilized as the radius vector in position 1 to determine the radius vector in position 2, with the values of the translation vector and rotation matrix calculated from the three forearm markers. This new radius vector in position 2 calculated with respect to the FUM calibration marker (defined as calibration point) in position 1 is found to be similar to the traced FUM marker trajectory obtained from the data acquisition system.

Figure 4.43, 4.44 and 4.45 shows clearly the comparison between the traced FUM marker trajectory values and the calculated values, along the X, Y and Z axes respectively for the forearm movement. From the graphs we find that there is very negligible variation between the traced FUM marker values and the calculated values.

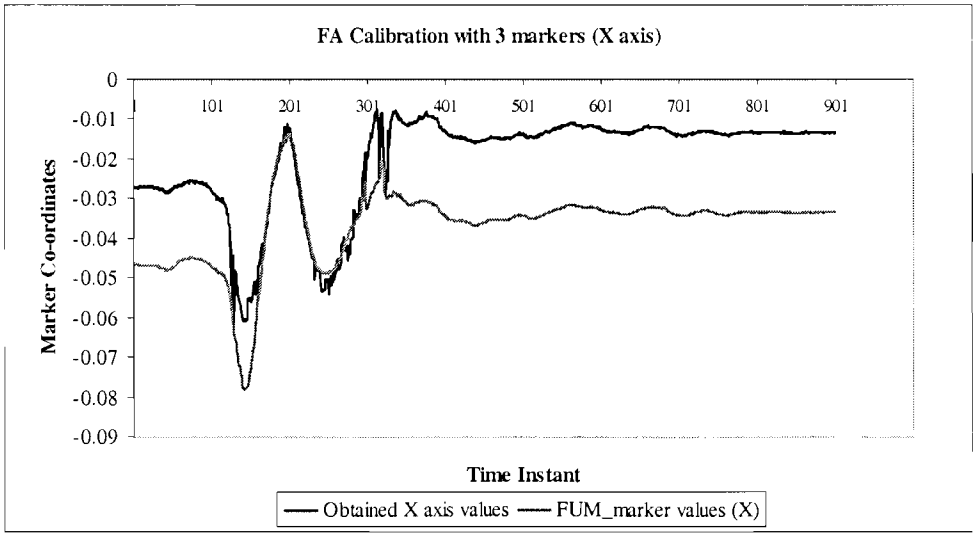

Figure 4.43. Comparison of traced FUM marker X-axis values and determined X-axis values relative to the calibration position for the forearm.

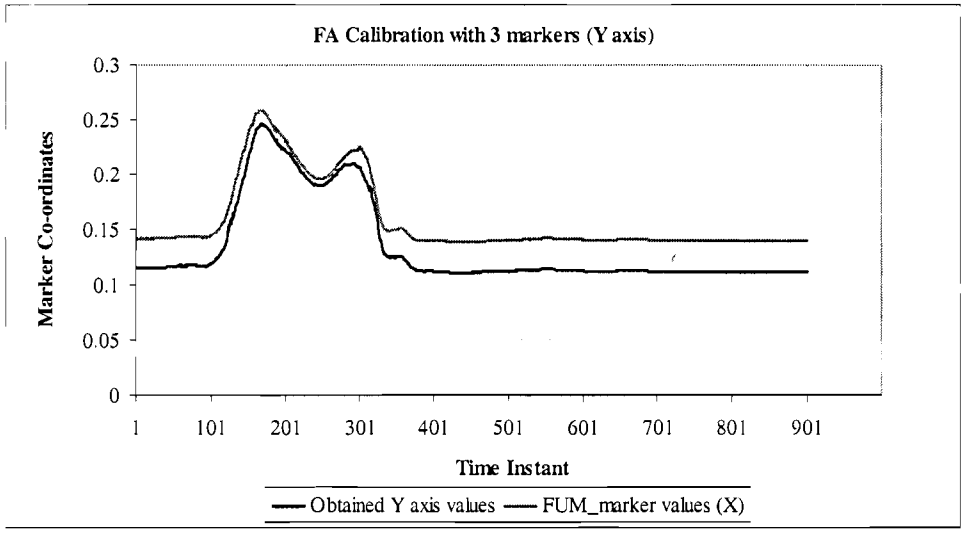

Figure 4.44. Comparison of traced FUM marker Y-axis values and determined Y-axis values relative to the calibration position for the forearm.

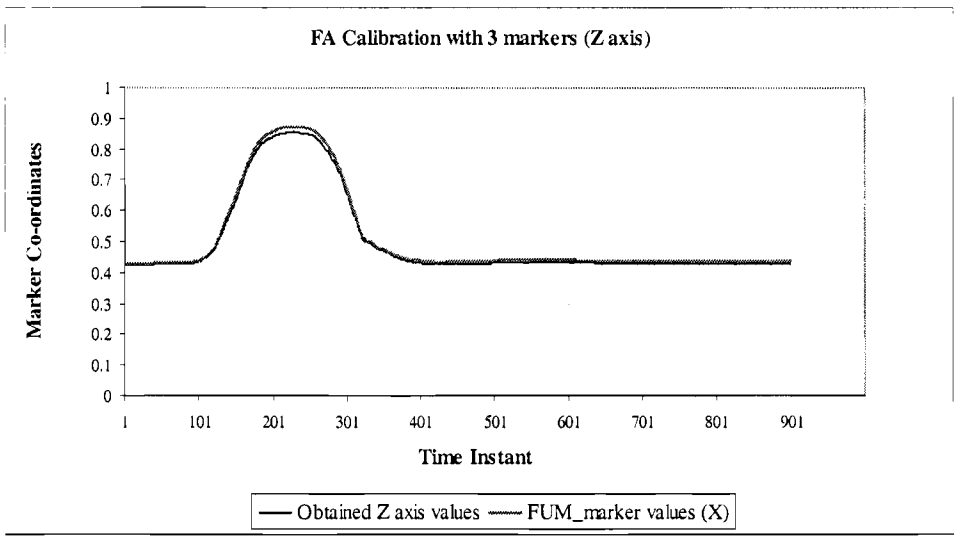

Figure 4.45. Comparison of traced FUM marker Z-axis values and determined Z-axis values relative to the calibration position for the forearm.

4.4.2.2 Relative to Previous Position with Averaging Compensation

On implementing this same approach of utilizing three markers and determining the trajectory, relative to the previous position with averaging compensation, it is found that the calculated values follow the same trajectory pattern as the pre-determined FUM marker. This is shown in figures 4.46, 4.47 and 4.48.

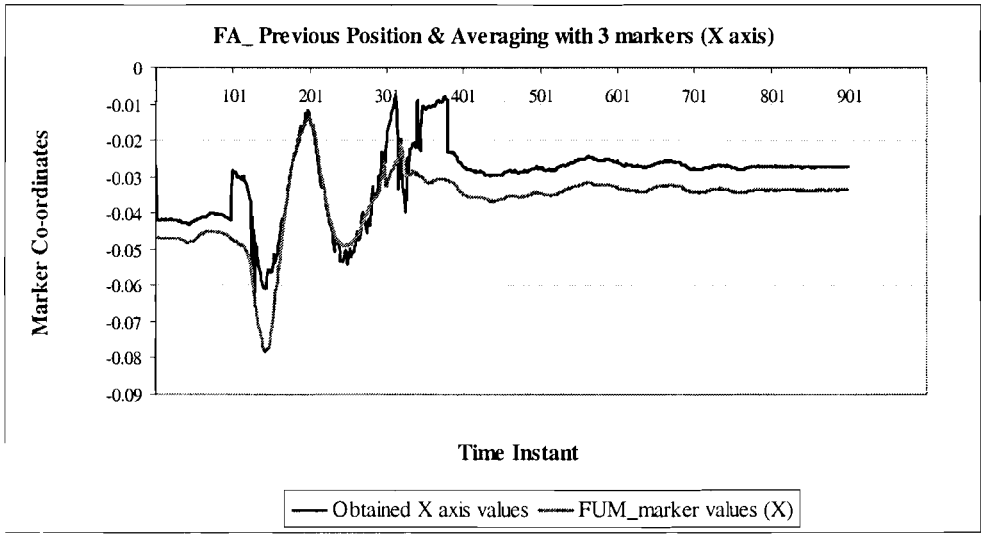

Figure 4.46 Comparison of traced FUM marker X-axis values and determined X-axis values relative to the previous position with averaging compensation for the forearm.

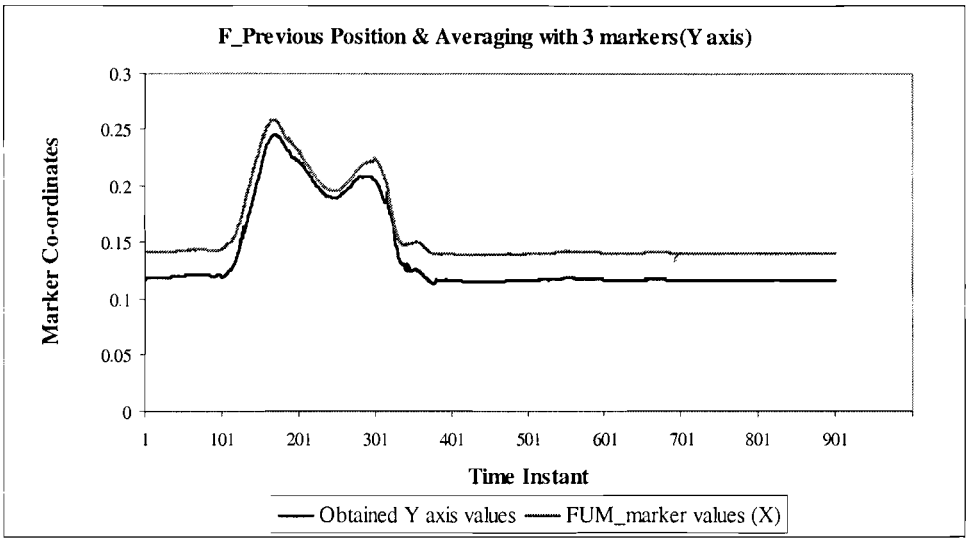

Figure 4.47 Comparison of traced FUM marker Y-axis values and determined Y-axis values relative to the previous position with averaging compensation for the forearm.

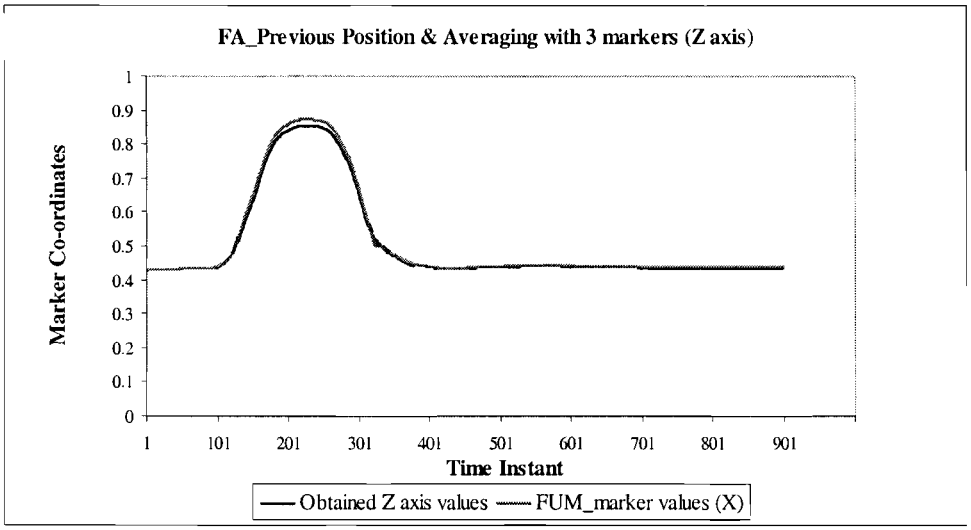

Figure 4.48 Comparison of traced FUM marker Z-axis values and determined Z-axis values relative to the previous position with averaging compensation for the forearm.

4.5. Possible Errors

The number of markers placed on the body for the study is one of the essential parameters in analyzing motion [Schmidt, R., et. al. 1999]. The minimum requirement for the number of non-collinear markers has been found to be three based on previous study [Challis, J. H., 1995]. However varying the number of markers can lead to slight variations in determining the values of the ideal translation vector and the rotation matrix of motion. As mentioned above, data was collected considering four markers and then analyzed to obtain the required kinematic parameters. The human body is considered as a rigid body for all these biomechanical calculations. However we find that the rigid shape is not maintained primarily because the skin and soft tissue movement cause displacements as large as 2cm between a marker and its corresponding anatomical landmark. There are physical and numerical solutions to this problem [Cheze, L. et. al. 1995]. The physical solution is to mount the markers on the rigid body and securely strapping it to the body segment. The advantage of this method is that the rigid body theory can be applied unambiguously to calculate segmental kinematics from the measured marker coordinates.

The major drawback of this method is that the rigid object is often strapped over a moving muscle mass rather than over anatomical landmarks with little intervening soft tissue. As a result soft tissue interference between the markers and the bone introduces motion disturbances which increase with distance from the bones. These motion

deviations cannot be easily eliminated by low pass filtering since their frequency is quiet close to the motion frequency.

The other numerical solution to compensate for soft tissue movement is the minimization of least square method adopted in this project to provide a best fit for translation vector v and rotation matrix T. The advantage here is that the individual markers can be mounted over anatomical landmarks with little intervening soft tissue, thus minimizing soft tissue motion disturbances and enhancing the accuracy of the kinematic calculations. The major disadvantage is that the results are purely numerical because the rigid body theory cannot be applied to calculate the required kinematic parameters (e.g screw axis parameters) between any pair of images.

4.6. Discussion

Kinetic data such as joint moments are significant for research and clinical applications in human motion analysis. They can offer the researcher and the clinician useful information that is essential in understanding the biomechanics of human movement and also is assessing the biomechanics of various clinical pathologies.

The accuracy of the Visual 3D program is verified, by comparing the elbow and wrist locations obtained from the designed computations, to the Visual 3D values, during a forward reaching movement of the subject. There is found to be a good co-relation between the two values. As shown in figures 4.10, 4.11 and 4.12, with respect to the

upper arm markers, the elbow locations obtained by calculating the next position relative to the previous position and then providing an averaging compensation perfectly correlates with the Visual 3D output, closely followed by method 2 of determining the elbow position relative to the calibration point. This is found to have a better correlation than that calculated relative to the previous position or by providing an extra identity rotation.

Similarly in order to determine the elbow position from the forearm markers, the output obtained by calculating the next position relative to the previous position and then providing an averaging compensation perfectly correlates with the Visual 3D output. Thus we find that the best method to determine the elbow location from markers is to calculate it relative to the previous position and provide an averaging compensation in case of oscillations. However, we find that the wrist position is best determined from the forearm markers, by calculating it relative to the calibration point. The accuracy of the Visual 3D software is finally best verified when three markers are utilized to determine the trajectory of the fourth marker. The computed trajectory of the fourth marker follows the same trend as the recorded original trajectory and the Visual 3D estimate, thus substantiating its exactness. The accuracy of the computed algorithm can be further compared with Visual 3D and tested using markers placed on a phantom arm.

This project can be further extended in order to avoid erroneous readings in case of marker drop outs and enable the computer simulation to use the connectivity of the

segments as additional information to determine the actual locations of the joint centers. Furthermore additional biomechanical parameters could also be calculated.

Literature Cited

Literature Cited

1. **Basmajian, J. V.**, *Therapeutic Exercise*, 3rd edition, Williams and Wilkins Publishing Co., 1978.

2. **Blin, O.,** Ferrandez, A.M., and Serratrice, G., Quantitative analysis of gait in Parkinson patients: Increased variability of stride length, *Journal of the Neurological Sciences*, Vol. 98, Issue 1, 91-97, 1990.

3. **Braune, W.,** Fischer, O., Die bei der Untersuchung von Gelenkbewegungen anzuwendende Methode, erlautet am Gelenkmechanismus des Vorderarms bei Menschen. Abh. d. Math.-Phys. Cl. d. k. Sachs. Gesellsch. d. Wissensch., 13:314,1885

4. **Brinckmann, Paul,** Frobin, Wolfgang, and Leivseth, Gunnar, *Musculoskeletal Biomechanics*, Thieme, Stuttgart, New York, 2000

5. **Cauchy, A-L.**, Exercises de Mathematiques, II. Paris, 1827.

6. **Challis John H.,** A procedure for determining rigid body transformation parameters. *Journal of Biomechanics*, Vol. 28, Issue 6, 733-737,1995

7. **Chao, E. Y.** and Morrey, B. F., Three-dimensional rotation of the elbow. *Journal of Biomechanics,* Vol. 11, 57-73, 1978.

8. **Chasles, M.,** Note sur les proprietes generales du systeme de deux corp semblables entr'eux. Bulletin Univ des Sciences, 14:321, 1830.

9. **Esch, D.** and Lepley, M., *Evaluation of Joint Motion: Methods of Measurement and Recording,* University of Minnesota, Minneapolis, MN 1974.

10. **Euler, L.,** Formulae generales pro translatione quacunque corporum rigidorum. Novi Comment Petrop 20:189, 1776. Reprinted in Euleri Opera Omnia (2), Basel 9:84, 1968.

11. **Gage, J.R.,** *Gait Analysis in Cerebral Palsy*. London: Mac Keith Press; 1991.

12. **Galley, P.M** and Forster, A.L., *Human Movement: An introductory text for physiotherapy students*, Churchill Livingston, 2nd Edition, Singapore, 1987.

13. **Harris, Gerald F.,** and Smith, Peter A., *Human Motion and Analysis: Current Applications and Future Directions*, New York: TAB-IEEE Press Books Series - Design and Applications; 1996.

14. **Hjortsjo, C-H.**, *Motion and movements*, Acta Univ Lund II 4, 1964.

15. **Hurley, G.R.,** McKenney, R., Robinson, M., Zadravec, M., and Pierrynowski, M.R., The role of the contra lateral limb in below-knee amputee gait. *Prosthetics and Orthotics International,* Vol. 14, Issue 1, 33-42, 1990.

16. **Ito, K.,** Ito, M., Motion control in living bodies and robots, *Society of Instrument and Control Engineers*, Tokyo, Japan, 1991.

17. **Kinzel, G. L.,** Hall, A. S. Jr. and Hillberry, B. M., Measurement of the total motion between two body segments-I. Analytical development. *Journal of Biomechanics*, Vol. 5, Issue 1, 93-105, 1972.

18. **Lew, W. D**. and Lewis, J. L., An anthropometric scaling method with application to the knee joint, *Journal of Biomechanics*, Vol. 10, Issue 3, 171-181,1977.

19. **MATLAB** User's Guide: Signal Processing Toolbox, Natick, MA: The Math Works Inc., 2003

20. **Maynard, F.M.,** Post –polio sequelae – Differential diagnosis and management, *Journal of the Neurological Sciences,* Vol. 8, Issue 3, 355-361, 1985.

21. **Muybridge, E.,** *The Human Figure in Motion,* New York, NY: Dover; Reprinted in 1955 from original volume published in 1887.

22. **Norkin, C.C.** and White, D.J., *Measurement of Joint Motion: A Guide to Goniometry*, F.A. Davis Co., Philadelphia, 1986.

23. **Olney, S.J.,** Griffin, M.P., Monga, T.N. and McBride, I.D., Work and power in gait of stroke patients, *Arch Phys Med Rehabil,* Vol. 72, 309-314, 1991.

24. **Olney, S.J.,** Monga T.N., and Costigan, P.A., Mechanical energy of walking of stroke patients, *Arch Phys Med Rehabil,* Vol. 67, Issue 2, 92-98, 1986.

25. **Perry, J.,** *Gait Analysis: Normal and Pathological Function.* Thorofare, NJ: Slack, Inc.; 1992.

26. **Rodrigues, O.,** Des lois geometriques qui regissent les deplacements d'un solide dans l'espace. Journal of Math, 5:380, 1840.

27. **Schmidt, R.,** Disselhorst-Klug, C., Silny, J. and Rau, G., A marker base measurement procedure for unconstrained wrist and elbow motions. *Journal of Biomechanics,* Vol. 32, Issue 6, 615-621, 1999

28. **Selvik, G.,** A roentgen Stereophotgrammetric method for the study of the kinematics of the skeletal system. *Acta Orthop Scand,* Volume 60, Supplement 232, 1-51, 1989.

29. **Spoor, C.W.** and Veldpaus, F. E., Rigid body motion calculated from spatial co-ordinates of markers, *Journal of Biomechanics*, Vol. 13, Issue 4, 391-393, 1980

30. **Steindler, A.,** *Kinesiology of the Human Body.* Springfield, III: 1970, Charles C Thomas Publisher, 1970: 631,632.

31. **Thomas, S.E,** Mazur J.M., Child M.E., and Supan, T.J., Quantitative evaluation of AFO use with myelomeningocele children, *Zeitschrift fur Kinderchirurgie (Stuttgart),* Vol. 44 (Supplement 1): 38-40, 1989.

32. **Trew, Marion,** and Everett Tony, Biomechanics, *Human Movement: An Introductory text*, Churchill Livingstone, New York, 1997.

33. **Veldpaus, F. E.,** Woltring, H. J. and Dortmans, L. L. M. G., A least-squares algorithm for the equiform transformation from spatial marker co-ordinates, *Journal of Biomechanics*, Vol. 21, Issue 1, 45-54, 1988

34. **Whittle, M.,** *Gait Analysis: An Introduction*, Oxford, England: Butterworth – Heinemann Ltd; 1991.

35. **Woltring, H.J.,** and Huiskes, R., Stereo photography. In: *Biomechanics of Human Movement: Application in Rehabilitation, Sports and Ergonomics.* Worthington, Ohio: Bertec Corporation; 263-274, 1990.

36. http://www.nationmaster.com/encyclopedia/Classical-mechanics

37. http://www.cmotion.com/products/visual3d/Visual3DOverview.htm

Appendices

Appendix A

Anatomical Background

This appendix describes the mechanics involved in normal human motion/gait. A vivid description of the musculature and joint rotation is given for normal human locomotion.

Musculoskeletal Basis for Movements

The frame work of the body consists of bones articulating at the joints. It is at the joints that motion takes place. A joint is defined as the junction between two bones. The hard core for the various bone segments moving around the joints is the bones. Each bone segment's mass is completed by soft tissue structures, such as muscles, connective tissues, blood vessels, nerves and skin.

There are eight principal body segments namely:

1) Axial Skeleton
    a) Head – Neck
    b) Trunk
2) Upper Extremity
    a) Arm
    b) Forearm
    c) Hand
3) Lower Extremity

a) Thigh

b) Leg

c) Foot

Upper Limb Movements

All movements are conventionally described as being initiated from the anatomical position. Motion at any joint in the body can be described as taking place in one of the three cardinal planes of the body (sagittal, frontal and transverse) around the three corresponding axes (coronal, anterior-posterior and longitudinal) [Esch, D., et. al.1974]. As shown in Figure A.1, these three cardinal planes:

1. Divide the body into equal parts.
2. Lie at right angles to each other.
3. Intersect at the center of gravity of the body.

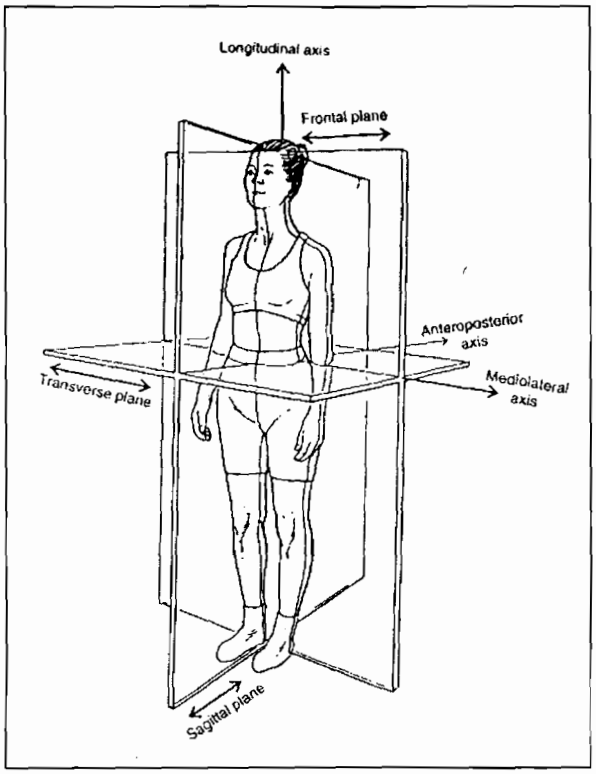

Figure A.1 Different planes of the human body

The three cardinal planes are [Galley, P.M. et. al. 1987];

1. Cardinal Sagittal Plane

It is a vertical plane extending from the anterior to posterior aspect of the body and dividing the body into equal right and left halves . Any plane parallel to this is called sagittal plane. As shown in Figure A.2, movement in a sagittal plane takes place about a frontal/coronal axis.

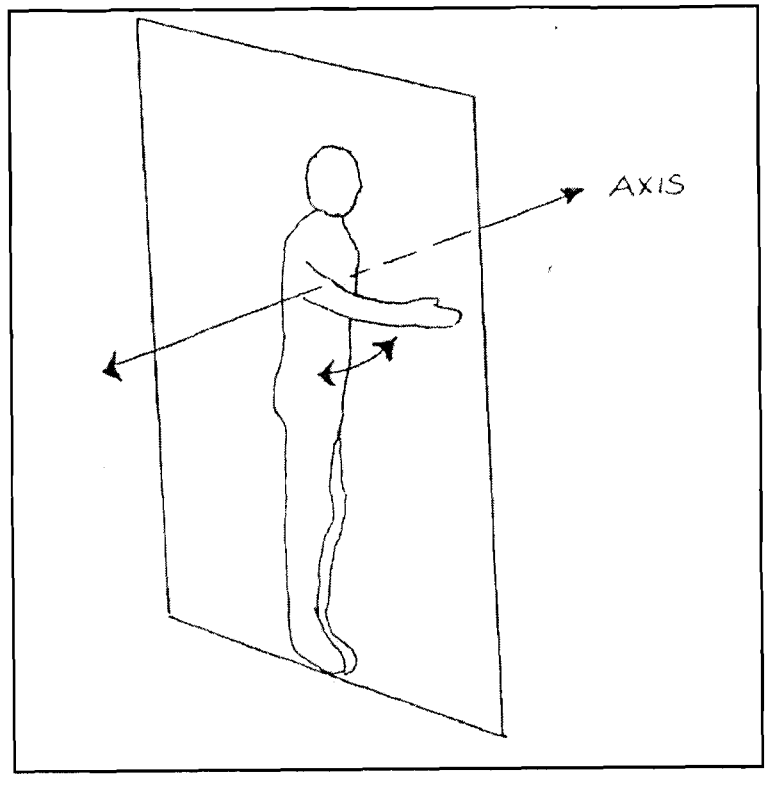

Figure A.2 Sagittal Plane showing extension and flexion

2. Cardinal Frontal Plane (sometimes called Coronal Plane)

It is a vertical plane extending from one side of the body to the other and dividing the body into equal front and back halves. Any plane parallel to this is called frontal plane. Movement in a frontal plane takes place about a sagittal/anterior-posterior axis. As shown in Figure A.3, the motion that occurs here are abduction and adduction of the hand/upper limb.

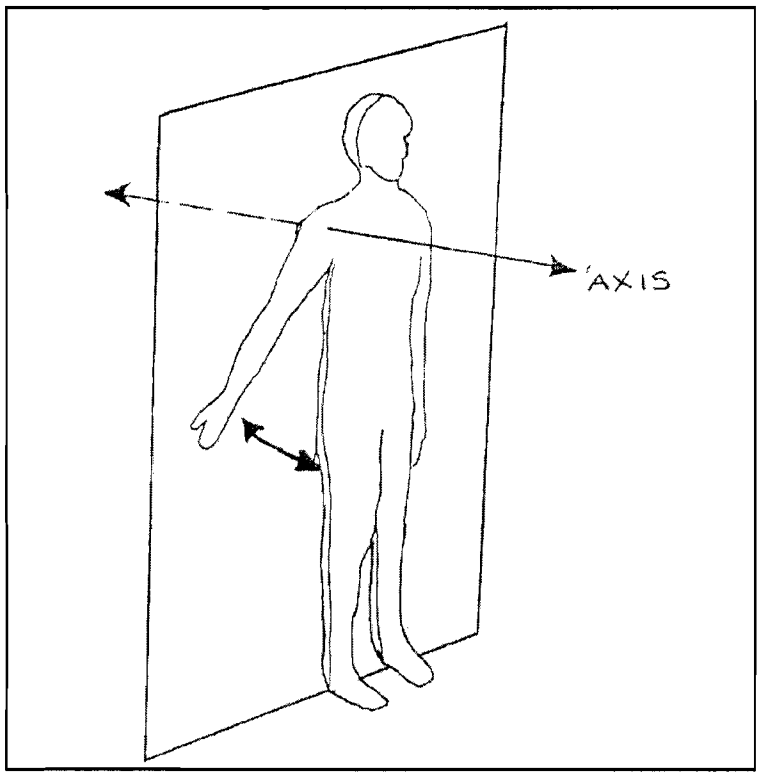

Figure A.3 Frontal Plane showing abduction and adduction

3. Cardinal Transverse Plane (sometimes called Horizontal Plane)

It is a horizontal plane dividing the body into equal upper and lower halves. Any plane parallel to this is called transverse plane. As shown in Figure A.4, movement in a transverse plane takes place about a vertical/longitudinal axis. Medial and lateral rotations occur in this plane.

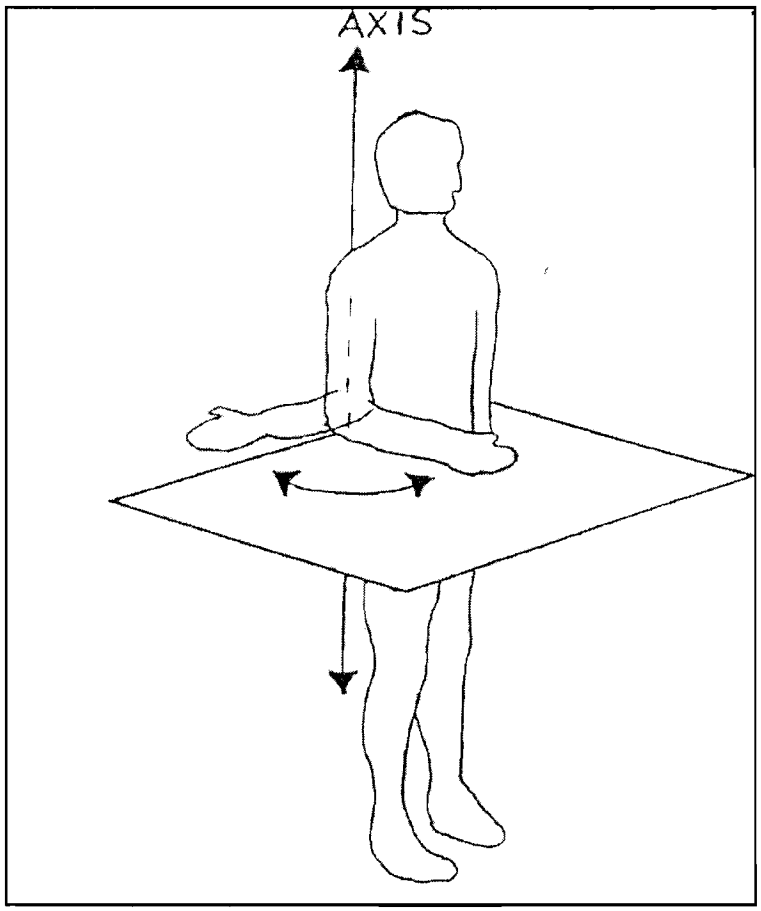

Figure A.4 Transverse plane showing internal/ external rotation

The major movements can be described as:

1. Movements in a sagittal plane about a frontal axis that are best observed from the side.
    a) Flexion, in which the angle between the surfaces of two adjacent segments decreases as the joint is bend.
    b) Extension, in which the angle between the segments increases. It is the opposite movement to flexion. An exception to this is the flexion and extension of the thumb that takes place in a frontal plane.

c) Dorsiflexion, where the foot is drawn towards the leg.

d) Plantar flexion, where the foot moves downwards from the leg.

2. Movements in a frontal plane about a sagittal axis that are best observed from behind or standing before the subject.

   a) Abduction, in which the segments moves away from the midline of the body.

   b) Adduction, in which the segment moves towards the midline of the body.

   c) Ulnar deviation, in which the hand moves in the direction of the little finger at the wrist.

   d) Radial deviation, in which the hand moves in the direction of the thumb at the wrist.

   e) Lateral flexion, of the trunk or head and neck in the right or the left direction.

3. Movements in a horizontal plane about a vertical axis.

   a) Medial (internal) rotation, in which the anterior surface of the segment turns inwards - towards the midline.

   b) Lateral (external) rotation, in which the anterior surface of the segment turns outwards - away from the midline.

   c) Rotation to the left or right of the vertebral column.

d) Supination, in which the hand is in anatomical position with reference to the forearm.

e) Pronation, in which the palm of the hand is turned away from the anatomical position so that it faces posterior.

4. Circumduction, in which a combination of the movements, flexion, abduction, extension and adduction is performed in sequence, so that the segment traces out a peculiar shape in space.

Appendix B

MATLAB Program Codes

All the codes written to test the accuracy of the biomechanical modeling tool were written in MATLAB, version 7.0. This appendix includes a listing of some of the codes written for the upper arm with elbow as the joint center of motion and the reverification using three markers.

1. Upper Arm_Elbow Relative to Calibration Position

```
n=4;

fid=fopen('c:\Project\data_excel
l\result\output.txt','w');

% Read Visual 3D File

VSX=xlsread('c:\Project\data_exc
ell\joint
centers\flex1_A_dist.xls','B2:B9
01');
VSY=xlsread('c:\Project\data_exc
ell\joint
centers\flex1_A_dist.xls','C2:C9
01');
VSZ=xlsread('c:\Project\data_exc
ell\joint
centers\flex1_A_dist.xls','D2:D9
01');

% Read in Calibration Data

A1=xlsread('c:\Project\data_exce
ll\static
calib\ALL_cal.xls','A1:C1');
A2=xlsread('c:\Project\data_exce
ll\static
calib\ALM_cal.xls','A1:C1');
A3=xlsread('c:\Project\data_exce
ll\static
calib\AUL_cal.xls','A1:C1');
A4=xlsread('c:\Project\data_exce
ll\static
calib\AUM_cal.xls','A1:C1');

% Average Elbow Position as
Calibration Point

wa=xlsread('c:\Project\data_exce
ll\static
calib\celbow_avg.xls','L3:N3');
 wa1=wa';

% Read in Trajectory Data

Q1=xlsread('c:\Project\data_exce
ll\marker\ALL_marker.xls','A1:C9
00');
Q2=xlsread('c:\Project\data_exce
ll\marker\ALM_marker.xls','A1:C9
00');
Q3=xlsread('c:\Project\data_exce
ll\marker\AUL_marker.xls','A1:C9
00');
Q4=xlsread('c:\Project\data_exce
ll\marker\AUM_marker.xls','A1:C9
00');
q=zeros(3,4,900);

i=1;
    for j=1:900
        q(:,i,j)=Q1(j,:);
        q(:,i+1,j)=Q2(j,:);
        q(:,i+2,j)=Q3(j,:);
        q(:,i+3,j)=Q4(j,:);
        i=1;
    end

   ca=A1'+A2'+A3'+A4';
   a=(1/n).*ca;
   at=a';
   ta1=A1';
   ta2=A2';
   ta3=A3';
   ta4=A4';

   elbow=zeros(1000,3);

 for i=1:1:900

r=q(:,1,i)+q(:,2,i)+q(:,3,i)+q(:
,4,i);
     p=(1/n).*r;
     e=[p*at];

     u=q(:,1,i)*A1;
     x=q(:,2,i)*A2;
     y=q(:,3,i)*A3;
     z=q(:,4,i)*A4;
     m=u+x+y+z;

     M=[((1/n).*[m])-e];

     mt=M';
     sym=mt*M;
     [V,D]=eig(sym);
     Vnew=V;
```

```
    V(:,1)=Vnew(:,3);
    V(:,3)=Vnew(:,1);

    Dnew=D;
    D(1,1)=Dnew(3,3);
    D(3,3)=Dnew(1,1);

    vt=V';

    dd11=D(1,1);
    dd22=D(2,2);
    dd33=D(3,3);

    mul=M*V;

    m1(:,1)=mul(:,1);
    m2(:,1)=mul(:,2);
    m3(:,1)=mul(:,3);

    D11=sqrt(dd11);
    D22=sqrt(dd22);
    D33=sqrt(dd33);

    D1=1/D11;
    D2=1/D22;
    D3=1/D33;

% Consider D11 and D22

    f1=D1.*m1;
    f2=D2.*m2;
    f3=(D1*D2);
    c1=m1;
    c2=m2;
    c3=m3;
    f4=cross(c1,c2);
    f5=f3.*f4;
    T12=[f1 f2 f5]*vt;

% Calculate Translation Vector

  smallv12=[p-(T12*a)];

    q12=[[T12*wa1]+smallv12];
    newq12(:,1)=q12(1,1);
    newq12(:,2)=q12(2,1);
    newq12(:,3)=q12(3,1);
  elbow(i,:)=q12';
trans=(smallv12'*smallv12);
temp=sqrt(smallv12'*smallv12);

% Helical Angle Calculation

X=acos(1/2*(T12(1,1)+T12(2,2)+T1
2(3,3)-1));

Y=asin(1/2*sqrt(((T12(3,2)-
T12(2,3))^2+(T12(1,3)-
T12(3,1))^2+(T12(2,1)-
T12(1,2))^2)));

nn=1/sin(Y).*(1/2.*[T12(3,2)-
T12(2,3);T12(1,3)-
T12(3,1);T12(2,1)-T12(1,2)]);
% Unit Vector along Helical Axis

I=eye(3,3);

bb=1/2*(T12+T12')-cos(X)*I;

ss=cross(1/2.*nn,cross(nn,smallv
12))+sin(Y)/(2*(1-
cos(Y))).*cross(nn,smallv12);  %
Radius Vector of a Point on the
Helical Axis

t=nn'*smallv12;  % Translation
along Helical Axis

fprintf(fid,'%f %f %f %f %f %f
%f %f %f %f %f
%f\n',elbow(i,:),trans,X,Y,small
v12',nn);

end

% Plotting the Overlay of 3d
Values and Elbow

xaxis=xlsread('c:\Project\data_e
xcell\joint
centers\xaxis.xls','A1:A900');
plot(xaxis,elbow(1:900,1),xaxis,
VSX);
plot(xaxis,elbow(1:900,2),xaxis,
VSY);
plot(xaxis,elbow(1:900,3),xaxis,
VSZ);
fclose(fid);
```

2. Upper Arm_Elbow Relative to Previous Position

```
n=4;

fid=fopen('c:\Project\data_excell
\result\output.txt','w');

% Read Visual 3D File

VSX=xlsread('c:\Project\data_exce
ll\joint
centers\flex1_A_dist.xls','B2:B90
1');
VSY=xlsread('c:\Project\data_exce
ll\joint
centers\flex1_A_dist.xls','C2:C90
1');
VSZ=xlsread('c:\Project\data_exce
ll\joint
centers\flex1_A_dist.xls','D2:D90
1');

% Read in Static Calibration Data

A1=xlsread('c:\Project\data_excel
l\static
calib\ALL_cal.xls','A1:C1');
A2=xlsread('c:\Project\data_excel
l\static
calib\ALM_cal.xls','A1:C1');
A3=xlsread('c:\Project\data_excel
l\static
calib\AUL_cal.xls','A1:C1');
A4=xlsread('c:\Project\data_excel
l\static
calib\AUM_cal.xls','A1:C1');

% Average Elbow Position as
Calibration Point

wa=xlsread('c:\Project\data_excel
l\static
calib\elbow_avg.xls','L3:N3');
wa1=wa';

% Read in Trajectory Data

Q1=xlsread('c:\Project\data_excel
l\marker\ALL_marker.xls','A1:C900
');
Q2=xlsread('c:\Project\data_excel
l\marker\ALM_marker.xls','A1:C900
');
Q3=xlsread('c:\Project\data_excel
l\marker\AUL_marker.xls','A1:C900
');
Q4=xlsread('c:\Project\data_excel
l\marker\AUM_marker.xls','A1:C900
');
q=zeros(3,4,999);

i=1;
    for j=1:900
        q(:,i,j)=Q1(j,:);
        q(:,i+1,j)=Q2(j,:);
        q(:,i+2,j)=Q3(j,:);
        q(:,i+3,j)=Q4(j,:);
        i=1;
    end

   ca=A1'+A2'+A3'+A4';
   a=(1/n).*ca;
   at=a';
   ta1=A1';
   ta2=A2';
   ta3=A3';
   ta4=A4';

elbow=zeros(1000,3);

for i=1:1:900

   if i>1
     A1=q(:,1,i-1)';
     A2=q(:,2,i-1)';
     A3=q(:,3,i-1)';
     A4=q(:,4,i-1)';

     wa1=elbow(i-1,:)';  %
Assigning Calibration Value to
the Previous Position
     ca=A1'+A2'+A3'+A4';
     a=(1/n).*ca;
     at=a';
     ta1=A1';
     ta2=A2';
     ta3=A3';
     ta4=A4';
   end
```

```
r=q(:,1,i)+q(:,2,i)+q(:,3,i)+q(:,
4,i);
   p=(1/n).*r;
   e=[p*at];

   u=q(:,1,i)*A1;
   x=q(:,2,i)*A2;
   y=q(:,3,i)*A3;
   z=q(:,4,i)*A4;
   m=u+x+y+z;

   M=[((1/n).*[m])-e];

   mt=M';
   sym=mt*M;
   [V,D]=eig(sym);

   Vnew=V;
   V(:,1)=Vnew(:,3);
   V(:,3)=Vnew(:,1);

   Dnew=D;
   D(1,1)=Dnew(3,3);
   D(3,3)=Dnew(1,1);

   vt=V';

   dd11=D(1,1);
   dd22=D(2,2);
   dd33=D(3,3);

   mul=M*V;

   m1(:,1)=mul(:,1);
   m2(:,1)=mul(:,2);
   m3(:,1)=mul(:,3);

   D11=sqrt(dd11);
   D22=sqrt(dd22);
   D33=sqrt(dd33);

   D1=1/D11;
   D2=1/D22;
   D3=1/D33;

  % Consider column D11 and D22

  f1=D1.*m1;
  f2=D2.*m2;
  f3=(D1*D2);
  c1=m1;
  c2=m2;
  c3=m3;
  f4=cross(c1,c2);
  f5=f3.*f4;
  T12=[f1 f2 f5]*vt;

% Calculate Translation Vector

  smallv12=[p-(T12*a)];

    q12=[[T12*wa1]+smallv12];
    newq12(:,1)=q12(1,1);
    newq12(:,2)=q12(2,1);
    newq12(:,3)=q12(3,1);

    elbow(i,:)=q12';

trans=(smallv12'*smallv12);

temp=sqrt(smallv12'*smallv12);

% Helical Angle Calculation

X=acos(1/2*(T12(1,1)+T12(2,2)+T12
(3,3)-1));

Y=asin(1/2*sqrt(((T12(3,2)-
T12(2,3))^2+(T12(1,3)-
T12(3,1))^2+(T12(2,1)-
T12(1,2))^2)));
    nn=1/sin(Y).*(1/2.*[T12(3,2)-
T12(2,3);T12(1,3)-
T12(3,1);T12(2,1)-T12(1,2)]);   %
Unit Vector along Helical Axis

I=eye(3,3);

bb=1/2*(T12+T12')-cos(X)*I;

ss=cross(1/2.*nn,cross(nn,smallv1
2))+sin(Y)/(2*(1-
cos(Y))).*cross(nn,smallv12);  %
Radius Vector of a Point on the
Helical Axis

t=nn'*smallv12;  % Translation
along Helical Axis
```

```
fprintf(fid,'%f %f %f %f %f %f %f
%f %f %f %f
%f\n',elbow(i,:),smallv12',X,Y,nn
,trans);

end

% Plotting the Overlay of 3d
Values and Elbow

xaxis=xlsread('c:\Project\data_ex
cell\joint
centers\xaxis.xls','A1:A900');
plot(xaxis,elbow(1:900,1),xaxis,V
SX);
plot(xaxis,elbow(1:900,2),xaxis,V
SY);
plot(xaxis,elbow(1:900,3),xaxis,V
SZ);

fclose(fid);
```

```
3. Upper Arm_Elbow Relative to Previous Position with Identity Matrix
Compensation

n=4;

fid=fopen('c:\Project\data_excell
\result\output.txt','w');

% Read Visual 3D File

VSX=xlsread('c:\Project\data_exce
ll\joint
centers\flex1_A_dist.xls','B2:B90
1');
VSY=xlsread('c:\Project\data_exce
ll\joint
centers\flex1_A_dist.xls','C2:C90
1');
VSZ=xlsread('c:\Project\data_exce
ll\joint
centers\flex1_A_dist.xls','D2:D90
1');

% Read in Calibration Data

A1=xlsread('c:\Project\data_excel
l\static
calib\ALL_cal.xls','A1:C1');
A2=xlsread('c:\Project\data_excel
l\static
calib\ALM_cal.xls','A1:C1');
A3=xlsread('c:\Project\data_excel
l\static
calib\AUL_cal.xls','A1:C1');
A4=xlsread('c:\Project\data_excel
l\static
calib\AUM_cal.xls','A1:C1');

% Average Elbow position as
Calibration Point

wa=xlsread('c:\Project\data_excel
l\static
calib\celbow_avg.xls','L3:N3');
 wa1=wa';

% Read in Trajectory Data

Q1=xlsread('c:\Project\data_excel
l\marker\ALL_marker.xls','A1:C900
');
Q2=xlsread('c:\Project\data_excel
l\marker\ALM_marker.xls','A1:C900
');
Q3=xlsread('c:\Project\data_excel
l\marker\AUL_marker.xls','A1:C900
');
Q4=xlsread('c:\Project\data_excel
l\marker\AUM_marker.xls','A1:C900
');
q=zeros(3,4,900);

i=1;
    for j=1:900
        q(:,i,j)=Q1(j,:);
        q(:,i+1,j)=Q2(j,:);
        q(:,i+2,j)=Q3(j,:);
        q(:,i+3,j)=Q4(j,:);
        i=1;
    end

   ca=A1'+A2'+A3'+A4';
   a=(1/n).*ca;
   at=a';
   ta1=A1';
   ta2=A2';
   ta3=A3';
   ta4=A4';

   elbow=zeros(1000,3);

for i=1:1:900

   if i>1
     A1=q(:,1,i-1)';
     A2=q(:,2,i-1)';
     A3=q(:,3,i-1)';
     A4=q(:,4,i-1)';

     wa1=elbow(i-1,:)';  %
Assigning calibration value to
the previous position
     ca=A1'+A2'+A3'+A4';
     a=(1/n).*ca;
     at=a';
     ta1=A1';
```

```
      ta2=A2';
      ta3=A3';
      ta4=A4';
     end

r=q(:,1,i)+q(:,2,i)+q(:,3,i)+q(:,
4,i);
      p=(1/n).*r;
      e=[p*at];

      u=q(:,1,i)*A1;
      x=q(:,2,i)*A2;
      y=q(:,3,i)*A3;
      z=q(:,4,i)*A4;
      m=u+x+y+z;

      M=[((1/n).*[m])-e];

      mt=M';
      sym=mt*M;
      [V,D]=eig(sym);

      Vnew=V;
      V(:,1)=Vnew(:,3);
      V(:,3)=Vnew(:,1);

      Dnew=D;
      D(1,1)=Dnew(3,3);
      D(3,3)=Dnew(1,1);

     vt=V';

     dd11=D(1,1);
     dd22=D(2,2);
     dd33=D(3,3);

    mul=M*V;

    m1(:,1)=mul(:,1);
    m2(:,1)=mul(:,2);
    m3(:,1)=mul(:,3);

    D11=sqrt(dd11);
    D22=sqrt(dd22);
    D33=sqrt(dd33);

    D1=1/D11;
    D2=1/D22;
    D3=1/D33;

   % Consider column D11 and D22

   f1=D1.*m1;
   f2=D2.*m2;
   f3=(D1*D2);
   c1=m1;
   c2=m2;
   c3=m3;
   f4=cross(c1,c2);
   f5=f3.*f4;
   T12=[f1 f2 f5]*vt;

% Calculate Translation Vector

   smallv12=[p-(T12*a)];

   marker=0;
    if
((smallv12'*smallv12)>0.05)&&(i>1
)
       T12=eye(3,3);
       smallv12=[p-(T12*a)];
       marker=1;
    end

 q12=[[T12*wa1]+smallv12];
     newq12(:,1)=q12(1,1);
     newq12(:,2)=q12(2,1);
     newq12(:,3)=q12(3,1);

elbow(i,:)=q12';

trans=(smallv12'*smallv12);

temp=sqrt(smallv12'*smallv12);

% Helical Angle Calculation

X=acos(1/2*(T12(1,1)+T12(2,2)+T12
(3,3)-1));

Y=asin(1/2*sqrt(((T12(3,2)-
T12(2,3))^2+(T12(1,3)-
T12(3,1))^2+(T12(2,1)-
T12(1,2))^2)));
    nn=1/sin(Y).*(1/2.*[T12(3,2)-
T12(2,3);T12(1,3)-
T12(3,1);T12(2,1)-T12(1,2)]);   %
Unit Vector along Helical Axis

I=eye(3,3);
```

```
bb=1/2*(T12+T12')-cos(X)*I;

ss=cross(1/2.*nn,cross(nn,smallv1
2))+sin(Y)/(2*(1-
cos(Y))).*cross(nn,smallv12);    %
Radius Vector of a point on the
Helical Axis

t=nn'*smallv12;  % Translation
along Helical Axis

fprintf(fid,'%f %f %f %f
%f\n',elbow(i,:),trans,marker);

end

% Plotting the overlay of 3d and
elbow

xaxis=xlsread('c:\Project\data_ex
cell\joint
centers\xaxis.xls','A1:A900');
plot(xaxis,elbow(1:900,1),xaxis,V
SX);
plot(xaxis,elbow(1:900,2),xaxis,V
SY);
plot(xaxis,elbow(1:900,3),xaxis,V
SZ);

fclose(fid);
```

4. Upper Arm_Elbow Relative to Previous Position with Averaging Compensation

```
n=4;

fid=fopen('c:\Project\data_excell
\result\output.txt','w');

% Read Visual 3D File

VSX=xlsread('c:\Project\data_exce
ll\joint
centers\flex1_A_dist.xls','B2:B90
1');
VSY=xlsread('c:\Project\data_exce
ll\joint
centers\flex1_A_dist.xls','C2:C90
1');
VSZ=xlsread('c:\Project\data_exce
ll\joint
centers\flex1_A_dist.xls','D2:D90
1');

% Read in Calibration Data

A1=xlsread('c:\Project\data_excel
l\static
calib\ALL_cal.xls','A1:C1');
A2=xlsread('c:\Project\data_excel
l\static
calib\ALM_cal.xls','A1:C1');
A3=xlsread('c:\Project\data_excel
l\static
calib\AUL_cal.xls','A1:C1');
A4=xlsread('c:\Project\data_excel
l\static
calib\AUM_cal.xls','A1:C1');

% Average Elbow Position as
Calibration Point

wa=xlsread('c:\Project\data_excel
l\static
calib\celbow_avg.xls','L3:N3');
 wa1=wa';

% Read in Trajectory Data

Q1=xlsread('c:\Project\data_excel
l\marker\ALL_marker.xls','A1:C900
');
Q2=xlsread('c:\Project\data_excel
l\marker\ALM_marker.xls','A1:C900
');
Q3=xlsread('c:\Project\data_excel
l\marker\AUL_marker.xls','A1:C900
');
Q4=xlsread('c:\Project\data_excel
l\marker\AUM_marker.xls','A1:C900
');
q=zeros(3,4,900);

i=1;
    for j=1:900
        q(:,i,j)=Q1(j,:);
        q(:,i+1,j)=Q2(j,:);
        q(:,i+2,j)=Q3(j,:);
        q(:,i+3,j)=Q4(j,:);
        i=1;
    end

   ca=A1'+A2'+A3'+A4';
   a=(1/n).*ca;
   at=a';
   ta1=A1';
   ta2=A2';
   ta3=A3';
   ta4=A4';

   elbow=zeros(1000,3);

 for i=1:1:900

     if i>1
        A1=q(:,1,i-1)';
        A2=q(:,2,i-1)';
        A3=q(:,3,i-1)';
        A4=q(:,4,i-1)';

        wa1=elbow(i-1,:)';   %
Assigning Calibration Value to
the Previous Position
        ca=A1'+A2'+A3'+A4';
        a=(1/n).*ca;
        at=a';
        ta1=A1';
        ta2=A2';
        ta3=A3';
        ta4=A4';
     end
```

```
r=q(:,1,i)+q(:,2,i)+q(:,3,i)+q(:,
4,i);
        p=(1/n).*r;
        e=[p*at];

        u=q(:,1,i)*A1;
        x=q(:,2,i)*A2;
        y=q(:,3,i)*A3;
        z=q(:,4,i)*A4;
        m=u+x+y+z;

        M=[((1/n).*[m])-e];

        mt=M';
        sym=mt*M;
        [V,D]=eig(sym);

        Vnew=V;
        V(:,1)=Vnew(:,3);
        V(:,3)=Vnew(:,1);

        Dnew=D;
        D(1,1)=Dnew(3,3);
        D(3,3)=Dnew(1,1);

        vt=V';

        dd11=D(1,1);
        dd22=D(2,2);
        dd33=D(3,3);

        mul=M*V;

        m1(:,1)=mul(:,1);
        m2(:,1)=mul(:,2);
        m3(:,1)=mul(:,3);

        D11=sqrt(dd11);
        D22=sqrt(dd22);
        D33=sqrt(dd33);

        D1=1/D11;
        D2=1/D22;
        D3=1/D33;

    % Consider D11 and D22

        f1=D1.*m1;
        f2=D2.*m2;
        f3=(D1*D2);
        c1=m1;
        c2=m2;
        c3=m3;
        f4=cross(c1,c2);
        f5=f3.*f4;
        T12=[f1 f2 f5]*vt;

% Calculate Translation Vector

  smallv12=[p-(T12*a)];

        q12=[[T12*wa1]+smallv12];
        newq12(:,1)=q12(1,1);
        newq12(:,2)=q12(2,1);
        newq12(:,3)=q12(3,1);

        elbow(i,:)=q12';


trans(i)=(smallv12'*smallv12);

temp=sqrt(smallv12'*smallv12);

% Helical Angle Calculation

X=acos(1/2*(T12(1,1)+T12(2,2)+T12
(3,3)-1));

Y=asin(1/2*sqrt(((T12(3,2)-
T12(2,3))^2+(T12(1,3)-
T12(3,1))^2+(T12(2,1)-
T12(1,2))^2)));

nn=1/sin(Y).*(1/2.*[T12(3,2)-
T12(2,3);T12(1,3)-
T12(3,1);T12(2,1)-T12(1,2)]);   %
Unit Vector along Helical Axis

I=eye(3,3);

bb=1/2*(T12+T12')-cos(X)*I;

ss=cross(1/2.*nn,cross(nn,smallv1
2))+sin(Y)/(2*(1-
cos(Y))).*cross(nn,smallv12);  %
Radius Vector of a Point on the
Helical Axis

t=nn'*smallv12;  % Translation
along Helical Axis
```

```
 end

  % Averaging Compensation

    for i=2:2:900
        marker=0;
        if (trans(i)>0.05)&&(i>1)
        avg=0;
        avg=(elbow(i-
1,:)+elbow(i+1,:))/2;
        elbow(i,:)=avg;
        marker=1;

       else

elbow(i,:)=elbow(i,:);
       marker=0;
       end

fprintf(fid,'%f %f
%f\n',elbow(i,:));

end

% Plotting the Overlay of 3d and
Elbow

xaxis=xlsread('c:\Project\data_ex
cell\joint
centers\xaxis.xls','A1:A900');
plot(xaxis,elbow(1:900,1),xaxis,V
SX);
plot(xaxis,elbow(1:900,2),xaxis,V
SY);
plot(xaxis,elbow(1:900,3),xaxis,V
SZ);

fclose(fid);
```

```
5. Upper Arm Relative to Calibration Position With 3 Markers

n=3;

fid=fopen('c:\Project\data_excell
\result\output.txt','w');

% Read in Calibration Data

A1=xlsread('c:\Project\data_excel
l\static
calib\ALL_cal.xls','A1:C1');
A2=xlsread('c:\Project\data_excel
l\static
calib\ALM_cal.xls','A1:C1');
A3=xlsread('c:\Project\data_excel
l\static
calib\AUL_cal.xls','A1:C1');

% Static Calibration AUM Marker
as Calibration Point

wa=xlsread('c:\Project\data_excel
l\static
calib\AUM_cal.xls','A1:C1');
wa1=wa';

% Read in Trajectory Data

Q1=xlsread('c:\Project\data_excel
l\marker\ALL_marker.xls','A1:C900
');
Q2=xlsread('c:\Project\data_excel
l\marker\ALM_marker.xls','A1:C900
');
Q3=xlsread('c:\Project\data_excel
l\marker\AUL_marker.xls','A1:C900
');

q=zeros(3,4,900);

i=1;
for j=1:900
    q(:,i,j)=Q1(j,:);
    q(:,i+1,j)=Q2(j,:);
    q(:,i+2,j)=Q3(j,:);
    i=1;
end

   ca=A1'+A2'+A3';
   a=(1/n).*ca;
   at=a';

   ta1=A1';
   ta2=A2';
   ta3=A3';

  elbow=zeros(1000,3);

for i=1:1:900

r=q(:,1,i)+q(:,2,i)+q(:,3,i);
      p=(1/n).*r;
      e=[p*at];

      u=q(:,1,i)*A1;
      x=q(:,2,i)*A2;
      y=q(:,3,i)*A3;
      m=u+x+y;

      M=[((1/n).*[m])-e];

      mt=M';
      sym=mt*M;
      [V,D]=eig(sym);

      Vnew=V;
      V(:,1)=Vnew(:,3);
      V(:,3)=Vnew(:,1);

      Dnew=D;
      D(1,1)=Dnew(3,3);
      D(3,3)=Dnew(1,1);

      vt=V';

      dd11=D(1,1);
      dd22=D(2,2);
      dd33=D(3,3);

      mul=M*V;

      m1(:,1)=mul(:,1);
      m2(:,1)=mul(:,2);
      m3(:,1)=mul(:,3);

      D11=sqrt(dd11);
      D22=sqrt(dd22);
      D33=sqrt(dd33);

      D1=1/D11;
```

```
      D2=1/D22;
      D3=1/D33;

% Consider D11 and D22

      f1=D1.*m1;
      f2=D2.*m2;
      f3=(D1*D2);
      c1=m1;
      c2=m2;
      c3=m3;
      f4=cross(c1,c2);
      f5=f3.*f4;
      T12=[f1 f2 f5]*vt;

% Calculate Translation Vector

 smallv12=[p-(T12*a)];

 q12=[[T12*wa1]+smallv12];
     newq12(:,1)=q12(1,1);
     newq12(:,2)=q12(2,1);
     newq12(:,3)=q12(3,1);

 elbow(i,:)=q12';

temp=sqrt(smallv12'*smallv12);

trans=(smallv12'*smallv12);

% Helical Angle Calculation

X=acos(1/2*(T12(1,1)+T12(2,2)+T12
(3,3)-1));

Y=asin(1/2*sqrt(((T12(3,2)-
T12(2,3))^2+(T12(1,3)-
T12(3,1))^2+(T12(2,1)-
T12(1,2))^2)));

nn=1/sin(Y).*(1/2.*[T12(3,2)-
T12(2,3);T12(1,3)-
T12(3,1);T12(2,1)-T12(1,2)]);   %
Unit Vector along Helical Axis

I=eye(3,3);

bb=1/2*(T12+T12')-cos(X)*I;

ss=cross(1/2.*nn,cross(nn,smallv1
2))+sin(Y)/(2*(1-
cos(Y))).*cross(nn,smallv12);  %
Radius Vector of a Point on the
Helical Axis

t=nn'*smallv12;   % Translation
along Helical Axis

fprintf(fid,'%f %f %f
%f\n',elbow(i,:),trans);

end


fclose(fid);
```

```
6. Upper Arm Relative to Previous Position with Averaging Compensation
With 3 Markers

n=3;

fid=fopen('c:\Project\data_excell
\result\output.txt','w');

% Read in Calibration Data

A1=xlsread('c:\Project\data_excel
l\static
calib\ALL_cal.xls','A1:C1');
A2=xlsread('c:\Project\data_excel
l\static
calib\ALM_cal.xls','A1:C1');
A3=xlsread('c:\Project\data_excel
l\static
calib\AUL_cal.xls','A1:C1');

% Static Calibration FUM Marker
as Calibration Point

wa=xlsread('c:\Project\data_excel
l\static
calib\AUM_cal.xls','A1:C1');
wa1=wa';

% Read in Trajectory Data

Q1=xlsread('c:\Project\data_excel
l\marker\ALL_marker.xls','A1:C900
');
Q2=xlsread('c:\Project\data_excel
l\marker\ALM_marker.xls','A1:C900
');
Q3=xlsread('c:\Project\data_excel
l\marker\AUL_marker.xls','A1:C900
');

q=zeros(3,4,900);

i=1;
for j=1:900
    q(:,i,j)=Q1(j,:);
    q(:,i+1,j)=Q2(j,:);
    q(:,i+2,j)=Q3(j,:);
    i=1;
end

   ca=A1'+A2'+A3';
   a=(1/n).*ca;
   at=a';
   ta1=A1';
   ta2=A2';
   ta3=A3';

elbow=zeros(1000,3);

for i=1:1:900
    if i>1
       A1=q(:,1,i-1)';
       A2=q(:,2,i-1)';
       A3=q(:,3,i-1)';

    wa1=elbow(i-1,:)';  %
Assigning Calibration Value to
the Previous Position

     ca=A1'+A2'+A3';
     a=(1/n).*ca;
     at=a';
     ta1=A1';
     ta2=A2';
     ta3=A3';

   end


r=q(:,1,i)+q(:,2,i)+q(:,3,i);
      p=(1/n).*r;
      e=[p*at];

      u=q(:,1,i)*A1;
      x=q(:,2,i)*A2;
      y=q(:,3,i)*A3;
      m=u+x+y;

      M=[((1/n).*[m])-e];

      mt=M';
      sym=mt*M;
      [V,D]=eig(sym);

      Vnew=V;
      V(:,1)=Vnew(:,3);
      V(:,3)=Vnew(:,1);

      Dnew=D;
```

```
        D(1,1)=Dnew(3,3);
        D(3,3)=Dnew(1,1);

        vt=V';

        dd11=D(1,1);
        dd22=D(2,2);
        dd33=D(3,3);

        mul=M*V;

        m1(:,1)=mul(:,1);
        m2(:,1)=mul(:,2);
        m3(:,1)=mul(:,3);

        D11=sqrt(dd11);
        D22=sqrt(dd22);
        D33=sqrt(dd33);

        D1=1/D11;
        D2=1/D22;
        D3=1/D33;

 % Consider D11 and D22

        f1=D1.*m1;
        f2=D2.*m2;
        f3=(D1*D2);
        c1=m1;
        c2=m2;
        c3=m3;
        f4=cross(c1,c2);
        f5=f3.*f4;
        T12=[f1 f2 f5]*vt;


 % Calculate Translation Vector

   smallv12=[p-(T12*a)];

   q12=[[T12*wa1]+smallv12];
      newq12(:,1)=q12(1,1);
      newq12(:,2)=q12(2,1);
      newq12(:,3)=q12(3,1);

   elbow(i,:)=q12';

temp=sqrt(smallv12'*smallv12);
trans(i)=(smallv12'*smallv12);
```

```
% Helical Angle Calculation

X=acos(1/2*(T12(1,1)+T12(2,2)+T12
(3,3)-1));

Y=asin(1/2*sqrt(((T12(3,2)-
T12(2,3))^2+(T12(1,3)-
T12(3,1))^2+(T12(2,1)-
T12(1,2))^2)));

nn=1/sin(Y).*(1/2.*[T12(3,2)-
T12(2,3);T12(1,3)-
T12(3,1);T12(2,1)-T12(1,2)]);   %
Unit Vector along Helical Axis

I=eye(3,3);

bb=1/2*(T12+T12')-cos(X)*I;

ss=cross(1/2.*nn,cross(nn,smallv1
2))+sin(Y)/(2*(1-
cos(Y))).*cross(nn,smallv12);  %
Radius Vector of a Point on the
Helical Axis

t=nn'*smallv12;  % Translation
along Helical Axis

end

% Averaging Compensation

 for i=3:2:900
     marker=0;
     if (trans(i)>0.05)
         avg=0;
         avg=(elbow(i-
1,:)+elbow(i+1,:))/2;
         elbow(i,:)=avg;
         marker=1;
     else

elbow(i,:)=elbow(i,:);
         marker=0;
     end

fprintf(fid,'%f %f
%f\n',elbow(i,:));
     end

fclose(fid);
```

Appendix C

Glossary

1. **Cerebral Palsy**: Condition developing in childhood due to unknown reasons manifesting with subnormal IQ and social functioning.

2. **Hemiplegia**: Weakness of right or left half of the body.

3. **Diplegia**: Weakness in lower half of the body.

4. **Spastic Hemiplegia**: Weakness of left or right half of the body with increased muscle tone.

5. **Parkinson's disease**: Neurologic condition due to dopamine deficiency causing paucity of movements, tremors and rigidity.

6. **Huntington's disease**: Genetic condition causing cognitive deficits beginning in 3rd- 4th decade resulting in death by the 5th decade.

7. **Chorea**: Spasmodic movements of body and limbs.

8. **Ataxia**: An inability to coordinate muscle activity during voluntary movement, so that smooth movements occur, most often due to disorders of the cerebellum or the posterior columns of the spinal cord; may involve the limbs, head, or trunk.

9. **Myelomeningocele**: Protrusion of the spinal cord covered in a meningeal sac filled with CSF from an unfused vertebral column.

10. **Stroke**: Neurological deficit subsequent to cellular insult, most commonly ischaemic, haemorrhagic or post-ictal.

11. **Post polio sequelae**: Residual neuromuscular damage and wasting after polio.